



Published in final edited form as:

Eur J Med Chem. 2020 October 15; 204: 112626. doi:10.1016/j.ejmech.2020.112626.

Novel HIV-1 Capsid-Targeting Small Molecules of the PF74 Binding Site

Lei Wang^{a,§}, Mary C. Casey^b, Sanjeev Kumar V. Vernekar^a, Rajkumar Lalji Sahani^a, Jayakanth Kankanala^a, Karen A. Kirby^c, Haijuan Du^c, Atsuko Hachiya^d, Huanchun Zhang^c, Philip R. Tedbury^c, Jiashu Xie^a, Stefan G. Sarafianos^c, Zhengqiang Wang^{*,a}

^aCenter for Drug Design, College of Pharmacy, University of Minnesota, Minneapolis, MN 55455, USA

^bDepartment of Molecular Microbiology and Immunology, University of Missouri School of Medicine, Christopher S. Bond Life Sciences Center, Columbia, MO 65211, USA

^cLaboratory of Biochemical Pharmacology, Department of Pediatrics, Emory University School of Medicine, Atlanta, GA 30322, USA

^dClinical Research Center, Nagoya Medical Center, National Hospital Organization, Nagoya, Aichi 460-0001, Japan

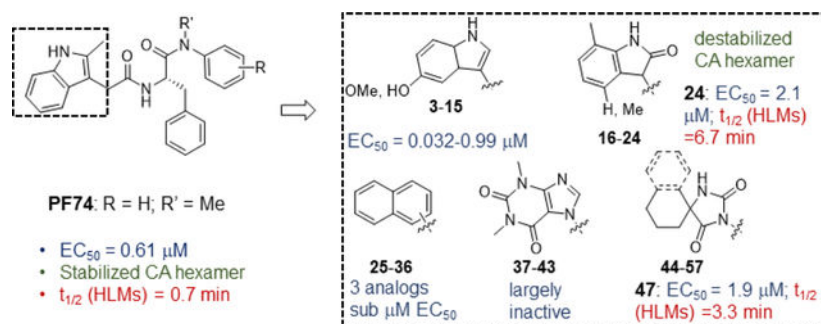
Abstract

The **PF74** binding site in HIV-1 capsid protein (CA) is a compelling antiviral drug target. Although **PF74** confers mechanistically distinct antiviral phenotypes by competing against host factors for CA binding, it suffers from prohibitively low metabolic stability. Therefore, there has been increasing interest in designing novel sub-chemotypes of **PF74** with similar binding mode and improved metabolic stability. We report herein our efforts to explore the inter-domain interacting indole moiety for designing novel CA-targeting small molecules. Our design includes simple substitution on the indole ring, and more importantly, novel sub-chemotypes with the indole moiety replaced with a few less electron-rich rings. All 56 novel analogs were synthesized and evaluated for antiviral activity, cytotoxicity, and impact on CA hexamer stability. Selected analogs were tested for metabolic stability in liver microsomes. Molecular modeling was performed to verify compound binding to the **PF74** site. In the end, 5-hydroxyindole analogs (**8,9** and **12**) showed improved potency (up to 20-fold) over **PF74**. Of the novel sub-chemotypes, α - and β -naphthyl analogs (**33** and **27**) exhibited sub micromolar antiviral potencies comparable to that of **PF74**. Interestingly, although only moderately inhibiting HIV-1 (single-digit micromolar EC₅₀s), analogs of the 2-indolone sub-chemotype consistently lowered the melting point (T_m) of CA hexamers, some with improved metabolic stability over **PF74**.

Graphical Abstract

*Corresponding Author: Zhengqiang Wang, Ph.D. wangx472@umn.edu; Phone: +1 (612) 626-7025.

§Present address: Department of Pharmacy, School of Chemical Engineering, Dalian University of Technology, Dalian 116024, China



Keywords

HIV-1; capsid-targeting antivirals; PF74; metabolic stability

1. Introduction

Although dozens of antivirals and fixed dose combinations [1] have been approved to treat the infection of human immunodeficiency virus type 1 (HIV-1), these drugs are not curative and HIV-1 remains a global healthcare challenge. Managing HIV-1 infection requires lifelong treatment, and hence, the virus will eventually develop resistance to current drug classes. Combating resistant viruses entails antivirals with novel molecular targets. The multifunctional HIV-1 capsid protein (CA) [2–4], which is a key component of the HIV-1 gag polyprotein [5], represents an emerging and highly attractive target in HIV-1 drug discovery [6–8]. CA is the building block of the mature HIV-1 capsid core [9, 10], and core stability critically depends on CA-CA interactions. Disrupting these interactions in the early stages of viral replication can perturb core stability to result in premature uncoating, impaired reverse transcription, and loss of infection [11, 12]. In addition, CA also interacts with multiple cellular factors [13] including TRIM5 α [14, 15], cleavage and polyadenylation specific factor 6 (CPSF6) [16, 17], nucleoporins 153 [18–20] and 358 [21, 22] (NUP153, NUP358), MxB [23, 24], and Cyclophilin A (CypA) [25–27]. These CA-host interactions regulate multiple post entry events, such as uncoating, cytoplasmic trafficking, reverse transcription, nuclear transport, integration site distribution, and the evasion of innate immunity [28]. During the late stage of viral replication, CA-CA interactions also drive the assembly and maturation of new infectious viral particles [29]. Therefore, CA-targeting small molecules could confer both early and late stage antiviral phenotypes.

Efforts targeting HIV-1 CA have identified a few chemotypes with distinct binding sites (Figure 1) [6, 7, 33]. CA is highly helical consisting of an N terminal domain (CA_{NTD}) and a C terminal domain (CA_{CTD}) with a flexible linker in-between [30, 34, 35]. Although CA_{CTD}-targeting compounds, such as polypeptide CAI [32], arylquinazoline (AQ) [36], and the covalently binding ebselen [37], have been reported, considerably more efforts have been directed toward targeting CA_{NTD}. At the base of the CA_{NTD} is the binding site for three chemical classes represented by BM-4 [31], BD-3 [31] and CAP-1 [38]. Interestingly, the backbone of BM-4 is a benzoimidazole core flanked by a pyrazole ring and a phenyl ring (Figure 1B). However, when the flanking moieties are reversed, the resulting compound C-4

[39] binds to a completely different site near the top of the CA_{NTD} and around the base of the cyclophilin A binding loop [40] (Figure 1A). In general, compounds binding to these two sites perturbed CA assembly *in vitro* and moderately inhibited HIV-1 in cell culture [6]. There was no evidence that they act in the early steps of viral replication, and no direct evidence linking the antiviral activity to the targeting of CA. By contrast, by far the most interesting CA-targeting compounds are the three chemical classes that bind to the **PF74** binding site, which also include the BI compounds [41] and the GS-CA compounds [42] (Figure 1B). These compounds all inhibited HIV-1 at both the early and the late stages of viral replication. Not surprisingly, there appears to be a positive correlation between the antiviral potency and the structural complexity: the simplest BI compounds exhibited moderate (low micromolar) antiviral activity and the structurally highly complex GS-CA compounds demonstrated sub-nanomolar antiviral activity, whereas the structurally elaborate, yet highly synthetically accessible peptidomimetic **PF74** inhibited HIV-1 in the sub-micromolar range. The binding mode [30] and the activity profile [43, 44] of **PF74** have been particularly well-characterized, revealing a dual antiviral mechanism of action: at low concentrations **PF74** competes against host factors for capsid binding; at high concentrations it induces premature uncoating, and consequently, impairs reverse transcription [11].

The **PF74** binding pocket is lined with residues in H3 and H4 of the CA_{NTD} (cyan) and H8 and H9 of the adjacent CA_{CTD} (blue), where an extensive network of molecular interactions defines the **PF74** binding mode (Figure 2A) [30]. Structurally, **PF74** features a phenylalanine core, connected by an aniline moiety at the carboxylate end and an indole-3-acetic acid at the amino end (Figure 2B). Although all three components provide key molecular interactions for CA binding, the indole ring (boxed, Figure 2A) uniquely interacts with both the CA_{NTD} (via H-bond with Q63 and π -cation interaction with K70) and the adjacent CA_{CTD} (via Y169, R173 and K182) [30]. These interactions are lacking with the BI compounds, which do not have a structural equivalent to the indole moiety of **PF74**, likely accounting for their weaker antiviral potency. The core and the aniline moiety of **PF74** engage extensively with the CA_{NTD} [30] (Figure 2A): 1) the phenylalanine core forms two H-bonds with N57, and an additional one with K70; 2) the aniline moiety makes contact with N53 (via the N-methyl group) and A105, T107, and Y130 (via the phenyl ring); and 3) the phenyl ring of the phenylalanine core forms hydrophobic interactions with residues M66 and L69. Since the indole moiety provides the unique inter-domain binding interactions, there have been reported efforts replacing the indole moiety with a simpler and synthetically more accessible 1,2,3-triazole ring, though the replacement resulted in substantially decreased potency (by >10-fold) [45, 46]. However, a recent report showed that replacing the indole ring with a piperazinone moiety yielded compounds with better antiviral activity (up to 6-fold) than PF-74 [47]. We have previously conducted a comprehensive SAR on **PF74** with the synthesis of a large number of analogs [48], and have identified a structurally novel and metabolically stable CA-targeting small molecule [49]. In the current report, we describe our own efforts targeting the two-domain interactions (Figure 2B). We first synthesized a series of **PF74** analogs with a substituent on the indole ring, and then designed and synthesized analogs of a few novel sub-chemotypes, each featuring a distinct ring system to replace the indole. In the end, 56 analogs were synthesized and tested, many of

which demonstrated significant anti-HIV-1 activity and interesting effects on CA hexamer stability, and some exhibited improved metabolic stability over **PF74**.

2. Results and discussion

2.1 Chemistry

Briefly, commercially available (*tert*-butoxycarbonyl)-*L*-phenylalanine (**58**) was treated with various amines under a well-established method using T₃P or HATU as the coupling agent in the presence of DIPEA as base to afford **59**. After removal of Boc protecting group using TFA, amine salts **60** were obtained which were further reacted with commercially available acids **61** to produce analogs **1–57**. Details about the synthesis of **59** and **60** were described in the Supporting Information.

2.2 Biological assays and SAR

All analogs were first evaluated in a thermal shift assay, where the effect of a compound on protein stability was measured by the change in protein melting point compared to DMSO control (T_m). A positive value in T_m indicates a stabilizing effect and a negative value a destabilizing effect on the protein. Of note, the CA protein used in the thermal shift assay is in a covalently crosslinked hexameric state. Thus, the T_m values likely reflect local changes that may affect stabilization and exclude inter-hexamer effects, which are important correlates of overall capsid core stability. To simplify presentation of the data, we refer to the effects of these compounds as stabilization or destabilization of “CA hexamer.” All compounds were also screened at 20 μ M in a cell-based antiviral assay against HIV-1. Compounds demonstrating significant inhibition were then tested at 2 μ M. Promising compounds were further assessed in dose response fashion for antiviral EC₅₀ values. All compounds were also tested for cytotoxicity either by screening at 100 or 50 μ M, or determination of CC₅₀ values. For some compounds, % inhibition at two concentrations (2 μ M and 20 μ M) was reported instead of the EC₅₀. **PF74** was resynthesized and tested in these assays ($T_m = 7.4$ °C, EC₅₀ = 0.61 μ M, CC₅₀ = 76 μ M).

2.2.1. Substitutions at the indole (R¹ and R²) and aniline ring (R³)—This series features **PF74** analogs with the indole ring substituted (R¹) with an OMe (**3–7**) or an OH (**8–15**). It is noteworthy that all these analogs lack the methyl group at R² (R² = H). This is because when compared to **PF74** (R² = Me, $T_m = 7.4$ °C, EC₅₀ = 0.61 μ M) analog **2** (R² = H, $T_m = 6.1$ °C, EC₅₀ = 0.46 μ M) showed a largely comparable activity profile. Hence, the SAR within this series concerns mainly the effect of the H-bond enabling and electron donating groups at R¹, in combination with the substitution effects on the aniline ring (R³). Notably, an OMe substitution at R¹ by itself did not improve the activity profile (**3** vs **2**), though slight improvement was observed when R³ is a *para*-Cl. This chlorine effect was significant as revealed by the direct comparison between analogs **7** (R³ = 4-Cl, $T_m = 8.0$ °C, EC₅₀ = 0.31 μ M) and **3** (R³ = H, $T_m = 4.9$ °C, EC₅₀ = 0.56 μ M), possibly due to a halogen bond (see molecular modeling for similar analogs). Among the compounds, **8–15**, substituted at R¹ with OH, were found the most potent ones of the series. Particularly, analogs **8** (EC₅₀ = 0.053 μ M), **9** (EC₅₀ = 0.035 μ M) and **12** (EC₅₀ = 0.032 μ M) conferred up to ~20-fold higher potency than **PF74** (EC₅₀ = 0.61 μ M) and analog **2** (EC₅₀ = 0.46 μ M).

Furthermore, **9** ($CC_{50} > 100 \mu\text{M}$) and **12** ($CC_{50} > 100 \mu\text{M}$) showed lower toxicity than **PF74** ($CC_{50} = 76 \mu\text{M}$). These results suggest that an R^1 substituent capable of both H-bond donating and H-bond accepting (e.g. OH) confers better antiviral potency than does an H-bond accepting group (e.g. OMe). However, the significantly improved antiviral potency with **8**, **9** and **12** over **PF74** is not correlated with results from the thermal shift assay, where very similar T_m (6.3–6.8 °C for **8**, **9**, **12** vs 7.4 °C for **PF74**) was observed. It is possible that the afore-mentioned OH group could affect capsid assembly via unknown post-binding molecular mechanisms. In addition, **PF74** is known to inhibit both the early and the late stages of HIV-1 replication cycle. Mechanistic studies are currently underway to determine if the most potent compounds (e.g. **8**, **9**, **12**) from this series display similar antiviral profile.

2.2.2. Novel sub-chemotypes with indole bioisosteres (R^5) and modifications at the aniline ring (R^3 and R^4)

—Table 2 summarizes our SAR studies on a few novel sub-chemotypes featuring different ring structures as the indole replacement. The first new sub-chemotype includes nine analogs (**16–24**) in which the indole moiety is replaced by an indolin-2-one ring. The first four analogs (**16–19**) bear a 7-methyl group and the next five (**20–24**) are 4,7-dimethyl substituted. Two prominent SAR trends were observed: the additional 4-methyl group (**20–24**) led to improved antiviral potency (**20** vs **16**, **22** vs **19**, **23** vs **17**); and both 3-Cl and 4-Cl on the aniline moiety (R^3) also enhanced potency (**18** vs **16**, **24** / **23** vs **20**). A beneficial chlorine effect conferred by both a 3-Cl and a 4-Cl of the aniline moiety (R^3) was observed with this sub-chemotype only (see molecular modeling). With **PF74** and all other sub-chemotypes, only the 4-Cl is properly positioned for halogen bonding. Overall, analogs of this series exhibited low micromolar potencies, and more intriguingly, seem to destabilize the CA hexamer. The next series consists of twelve analogs (**25–36**) with the indole moiety replaced by a naphthyl ring, either via a β substitution (**25–30**) or an α substitution (**31–36**). The substitution site (β vs α) did not appear to impact antiviral activity (**32** vs **26**, **33** vs **27**) as prominently as the R^3 group, where a 4-Me (**26**) or 4-Cl (**27**) conferred submicromolar activities, though in the α series (**31–36**) two additional compounds (**31** and **36**, $R^3 = \text{H}$) also demonstrated low micromolar antiviral activity. Next we synthesized seven analogs (**37–43**) where R^5 is a 1,3-dimethyl-purine-2,6-dione ring system. Unfortunately, none of them inhibited HIV-1 significantly at 2 μM . Discernible impact on CA hexamer stability was not observed either. The last two sub-chemotypes (**44–57**) synthesized both feature a [6,5] spiro ring system. Overall, analogs of these two sub-chemotypes did not significantly impact CA hexamer stability. As for antiviral potency, while many of the bicyclic analogs (**44–53**) inhibited HIV-1, such as compounds **44**, **46**, **47**, **50**, and **53**, the four tricyclic analogs (**54–57**) did not show any antiviral activity.

2.3. Metabolic stability in liver microsomes

Despite its potent antiviral activity, well-characterized mode of binding and easy synthetic accessibility, **PF74** is seriously flawed as an antiviral lead due to its prohibitively poor metabolic stability. In human liver microsomes (HLMs), the half-life ($t_{1/2}$) of **PF74** was less than 1 min [46, 50]. We have previously tested around 20 **PF74** analogs in HLMs and they all showed very poor metabolic stability ($t_{1/2} = 0.6–2.1$ min) [48]. However, an analog featuring a quinazoline-2,4-dione as the indole replacement was found to be metabolically stable in HLMs ($t_{1/2} = 31$ min) [49]. To gauge the metabolic stability of the sub-chemotypes

described herein, we tested selected compounds in HLMs and mouse liver microsomes (MLMs) and the results are summarized in Table 3. Consistent with literature reports, the $t_{1/2}$ of **PF74** in our metabolic assays was 0.7 min in HLMs and 0.6 min in MLMs. Peptidomimetics, a compound class to which **PF74** belongs, are particularly liable toward phase I metabolism, presumably because they are good substrates for liver metabolizing enzyme subfamily cytochrome P450 3A (CYP3A) [51]. This extensive liver metabolism constitutes a major pharmacokinetic (PK) barrier for many FDA-approved HIV-1 protease inhibitors [52]. For example, darunavir was reported to have a half-life ($t_{1/2}$) of 3.6 min in a human liver microsomal incubation system with less CYP protein content compared to ours (0.1 mg/mL vs 0.5 mg/mL) [53]. The main mitigating strategy has been to co-administer the antiviral drugs with a CYP3A inhibitor, such as ritonavir [54] or Cobicistat (Cobi) [55], as a PK enhancer [52]. Therefore, our metabolic stability assays were performed under two distinct sets of conditions: with PK enhancer Cobi or without Cobi (Table 3). Without Cobi, **PF74** analogs (**3** and **7**) exhibited very short half-life (1.2 min and 1.8 min, respectively). The metabolic stability remained poor for analogs of novel sub-chemotypes, though a few of them, such as **16**, **24**, **37** and **46**, did show substantially (7 to 10-fold) improved half-life over **PF74** in HLMs. For the five selected compounds tested in the presence of PK enhancer Cobi, drastically improved metabolic stability was observed with all (Table 3). Collectively, these results demonstrated that replacement of the indole moiety with a less electron-rich ring could lead to metabolically more stable compounds, and that inhibiting CYP3A could mitigate the phase I metabolic liability of this type of compounds.

2.4 Molecular modeling

To evaluate the binding mode of the new analogs, we performed molecular modeling of key compounds based on the co-crystal structure of native HIV-1 capsid protein bound to **PF74** (PDB code: 4XFZ [30]). Analog **12** is found to orient in a similar fashion as the parent compound **PF74** (Figure 3A), and share common key interactions on CA_{NTD} domain including (i) hydrogen bonding with N57 via the carbonyl and NH of phenylalanine core, with Q63 via indole N-H, and with K70 via the other carbonyl moiety; (ii) Cation- π interaction with K70 via the indole moiety (Figure 3A). However, unlike **PF74**, the two additional substituents of **12**, 4-Cl on the aniline moiety and 5-OH of the indole ring, confer a halogen bond (pink dashed line) and another hydrogen bond with K182 on the adjacent CA_{CTD} domain (black dotted line), respectively (Figure 3A). These additional interactions are consistent with improved target binding affinity (Glide score: -7.6 kcal/mol for **12** vs -5.8 kcal/mol for **PF74**) and largely increased potency (EC_{50} : 0.032 μ M for **12** vs 0.61 μ M for **PF74**). Importantly, while the halogen bond conferred by the 4-Cl of the aniline moiety appeared to be less important for potency than the hydrogen bond by the 5-OH (**2** vs **8** vs **12**), moving the Cl from 4 position to 3 (compound **13**) led to a 10-fold potency drop, likely due to the potential steric clash posed by the 3-Cl. Similar effects were observed with 3-Br (**14**) and 3-CF₃ (**15**). The potency difference between 3-Cl and 4-Cl aniline analog was prominent throughout SAR studies (**27** vs **28**, **33** vs **34**, and **50** vs **51**). The only exception is with the 4,7-dimethylindolin-2-one sub-chemotype where a beneficial halogen effect was observed for both the 4-Cl analog **23** (Figure 3B) and the 3-Cl analog **24** (Figure 3C). In both cases, the loss of the key H-bonding with Q63 and the cation- π interactions with K70, was compensated by a halogen-bond (pink dashed line) with N74 (4-Cl) and N53 (3-Cl),

respectively. Similarly, compound **27** having the 2-naphthyl ring in place of indole ring exhibited an identical potency and protein binding affinity to **PF74**, despite the loss of a key hydrogen-bonding with Q63 (Figure 3D). Possible orientation of the aniline ring of the compound **27** as shown in Figure 3D could improve hydrophobic contacts with N53, G106, and Y130, as a result of halogen bond between G106 and 4-Cl aniline, and could explain the observed potency for this and another similar compound **33**.

3. Conclusions

In this work, we have designed, synthesized and evaluated 56 compounds consisting of **PF74** analogs and a few novel **PF74**-like chemotypes featuring rings less electron-rich than the indole ring. In the end, 5-hydroxyindole analogs (**8**, **9**, **12**) were up to 20-fold more potent than the prototype **PF74**. Analogues with low to sub micromolar antiviral activities were also identified from all sub-chemotypes, except for the 1,3-dimethyl-purine-2,6-dione sub-chemotype. Of all sub-chemotypes studied herein, the naphthalene ring conferred the best potency as both the α - and β -naphthyl analogs (**33** and **27**) exhibited antiviral potencies comparable to that of **PF74**. Interestingly, the 2-indolone sub-chemotype lowered the T_m of CA hexamers, indicating a unique HIV-1 CA-destabilizing mechanism. The best 2-indolone analog, **24**, also showed 10-fold longer half-life in HLMs than **PF74**. These findings necessitate future medicinal chemistry to further optimize these novel sub-chemotypes, particularly the CA-destabilizing 2-indolone chemotype.

4. Experimental section

4.1 Chemistry

General Procedures.—All commercial chemicals were used as supplied unless otherwise indicated. Flash chromatography was performed on a Teledyne Combiflash RF-200 with RediSep columns (silica) and indicated mobile phase. ^1H and ^{13}C NMR spectra were recorded on a Varian 600 MHz or Bruker 400 spectrometer. Diastereomeric ratio (dr) was determined by ^1H NMR analysis. Mass data were acquired using an Agilent 6230 TOF LC/MS spectrometer. All NMR and mass spectrometers are located in the shared instrument rooms at the Center for Drug Design, University of Minnesota.

4.1.1. Synthesis of 59 and 60—Synthesis of intermediates **59** and **60** are described in Supporting Information.

4.1.2. Synthesis of (S)-N-Methyl-2-(2-(2-methyl-1H-indol-3-yl)acetamido)-N,3-diphenylpropanamide (1)—To a solution of commercially available 2-(2-methyl-1H-indol-3-yl)acetic acid (100 mg, 0.53 mmol, 1 equiv.) in DMF (3 mL), HATU (402 mg, 1.06 mmol, 2 equiv.) and DIPEA (205 mg, 1.59 mmol, 3 equiv.) were added and the mixture was stirred at room temperature for 20 min before (*S*)-2-amino-*N*-methyl-*N*,3-diphenylpropanamide (TFA salt, 235 mg, 0.64 mmol, 1.2 equiv.) was added. The mixture was further stirred overnight at room temperature. Upon completion, H_2O was added and the reaction mixture was extracted with EtOAc (3×30 mL). The organic phases were combined and washed with brine, dried over anhydrous MgSO_4 , filtered and concentrated. The product was purified by Combiflash on silica gel using EtOAc/hexane (1:2 to 6:1) as eluent. Yield

70%. ^1H NMR (600 MHz, DMSO- d_6) δ 10.68 (s, 1H), 8.27 (d, J = 7.0 Hz, 1H), 7.38 (dd, J = 17.5, 6.5 Hz, 3H), 7.27 (dd, J = 18.7, 6.7 Hz, 3H), 7.18 (d, J = 7.6 Hz, 1H), 7.12 (s, 3H), 6.98 – 6.89 (m, 1H), 6.84 (d, J = 6.9 Hz, 1H), 6.79 (s, 2H), 4.41 (s, 1H), 3.51 – 3.31 (m, 2H), 3.15 (s, 3H), 2.82 (d, J = 11.5 Hz, 1H), 2.67 (d, J = 11.5 Hz, 1H), 2.23 (s, 3H); ^{13}C NMR (150 MHz, DMSO- d_6) δ 171.5, 171.0, 143.3, 138.0, 135.4, 133.3, 130.0, 129.2, 128.8, 128.4, 128.2, 128.0, 126.7, 120.3, 118.4, 118.4, 110.5, 105.3, 52.2, 37.6, 37.4, 31.3, 11.7; HRMS (ESI) m/z calcd for $\text{C}_{27}\text{H}_{26}\text{N}_3\text{O}_2$ $[\text{M} - \text{H}]^-$ 424.2031, found 424.2029.

(S)-2-(2-(1H-Indol-3-yl)acetamido)-N-methyl-N,3-diphenylpropanamide (2): The synthetic method was similar to that of compound **1** except that 2-(1*H*-indol-3-yl)acetic acid (100 mg, 0.57 mmol, 1 equiv.) and (*S*)-2-amino-*N*-methyl-*N*,3-diphenylpropanamide (TFA salt, 252 mg, 0.68 mmol, 1.2 equiv.) were used as starting materials. Yield 65%. ^1H NMR (600 MHz, CD_3OD) δ 7.42 (d, J = 7.9 Hz, 1H), 7.37 – 7.31 (m, 4H), 7.18 – 7.05 (m, 5H), 7.03 – 6.94 (m, 3H), 6.75 (d, J = 7.3 Hz, 2H), 4.66 (t, J = 7.2 Hz, 1H), 3.61 (dd, J = 22.4, 15.8 Hz, 2H), 3.16 (s, 3H), 2.87 (dd, J = 13.3, 6.6 Hz, 1H), 2.64 (dd, J = 13.3, 6.6 Hz, 1H); ^{13}C NMR (150 MHz, CD_3OD) δ 172.7, 171.7, 142.5, 136.7, 136.5, 129.4, 128.7, 128.0, 127.9, 127.2, 127.0, 126.4, 123.5, 121.1, 118.6, 118.0, 110.9, 107.7, 51.9, 37.7, 36.6, 32.2; HRMS (ESI) ($-$) m/z calcd for $\text{C}_{26}\text{H}_{24}\text{N}_3\text{O}_2$ $[\text{M} - \text{H}]^-$ 410.1874, found 410.1878.

(S)-2-(2-(5-Methoxy-1H-indol-3-yl)acetamido)-N-methyl-N,3-diphenylpropanamide (3): The synthetic method was similar to that of compound **1** except that 2-(5-methoxy-1*H*-indol-3-yl)acetic acid (100 mg, 0.49 mmol, 1 equiv.) and (*S*)-2-amino-*N*-methyl-*N*,3-diphenylpropanamide (TFA salt, 217 mg, 0.59 mmol, 1.2 equiv.) were used as starting materials. Yield 42%. ^1H NMR (600 MHz, CDCl_3) δ 8.34 (s, 1H), 7.36 – 7.31 (m, 3H), 7.26 – 7.24 (m, 1H), 7.13 (t, J = 7.4 Hz, 1H), 7.07 – 7.04 (m, 2H), 6.97 – 6.88 (m, 5H), 6.66 (d, J = 7.4 Hz, 2H), 6.30 (d, J = 8.0 Hz, 1H), 4.81 – 4.77 (m, 1H), 3.79 (s, 3H), 3.67 – 3.60 (m, 2H), 3.18 (s, 3H), 2.76 (dd, J = 13.3, 7.0 Hz, 1H), 2.56 (dd, J = 13.3, 7.1 Hz, 1H); ^{13}C NMR (150 MHz, CDCl_3) δ 171.3, 171.0, 154.4, 142.4, 136.0, 131.4, 129.7, 129.1, 128.3, 128.2, 127.4, 127.3, 126.7, 124.4, 113.0, 112.1, 108.4, 100.1, 55.8, 51.3, 38.8, 37.6, 33.3; HRMS (ESI) m/z calcd for $\text{C}_{27}\text{H}_{26}\text{N}_3\text{O}_3$ $[\text{M} - \text{H}]^-$ 440.1980, found 440.1983.

(S)-2-(2-(5-Methoxy-1H-indol-3-yl)acetamido)-N-methyl-3-phenyl-N-(p-tolyl)propanamide (4): The synthetic method was similar to that of compound **1** except that 2-(5-methoxy-1*H*-indol-3-yl)acetic acid (100 mg, 0.49 mmol, 1 equiv.) and (*S*)-2-amino-*N*-methyl-3-phenyl-*N*-(*p*-tolyl)propanamide (TFA salt, 225 mg, 0.59 mmol, 1.2 equiv.) were used as starting materials. Yield 63%. ^1H NMR (600 MHz, CDCl_3) δ 8.60 (s, 1H), 7.22 (d, J = 8.7 Hz, 1H), 7.13 – 7.12 (m, 3H), 7.08 – 7.05 (m, 2H), 6.88 – 6.69 (m, 7H), 6.33 (d, J = 8.2 Hz, 1H), 4.82 – 4.79 (m, 1H), 3.79 (s, 3H), 3.66 – 3.59 (m, 2H), 3.15 (s, 3H), 2.77 (dd, J = 13.3, 7.0 Hz, 1H), 2.58 (dd, J = 13.3, 6.9 Hz, 1H), 2.35 (s, 3H); ^{13}C NMR (100 MHz, CDCl_3) δ 171.5, 170.9, 154.3, 139.9, 138.1, 136.1, 131.5, 130.3, 129.2, 128.3, 127.4, 127.0, 126.7, 124.5, 112.8, 112.2, 108.2, 100.1, 55.8, 51.2, 38.8, 37.7, 33.4, 21.1; HRMS (ESI) m/z calcd for $\text{C}_{28}\text{H}_{28}\text{N}_3\text{O}_3$ $[\text{M} - \text{H}]^-$ 454.2136, found 454.2139.

(S)-N-(4-Fluorophenyl)-2-(2-(5-methoxy-1H-indol-3-yl)acetamido)-N-methyl-3-phenylpropanamide (5): The synthetic method was similar to that of compound **1** except

that 2-(5-methoxy-1*H*-indol-3-yl)acetic acid (100 mg, 0.49 mmol, 1 equiv.) and (*S*)-2-amino-*N*-(4-fluorophenyl)-*N*-methyl-3-phenylpropanamide (TFA salt, 228 mg, 0.59 mmol, 1.2 equiv.) were used as starting materials. Yield 62%. ¹H NMR (600 MHz, CD₃OD) δ 7.24 (d, *J* = 8.8 Hz, 1H), 7.17 – 7.12 (m, 3H), 7.06 (s, 1H), 7.01 – 6.98 (m, 3H), 6.86 – 6.76 (m, 5H), 4.57 (t, *J* = 7.4 Hz, 1H), 3.79 (s, 3H), 3.57 (s, 2H), 3.11 (s, 3H), 2.89 (dd, *J* = 13.3, 7.5 Hz, 1H), 2.67 (dd, *J* = 13.3, 7.3 Hz, 1H); ¹³C NMR (150 MHz, CD₃OD) δ 174.15, 173.20, 163.35 (d, *J*_{CF} = 246.9 Hz), 155.20, 139.96, 137.82, 133.26, 130.67 (d, *J*_{CF} = 7.8 Hz), 130.19, 129.50, 128.75, 127.92, 125.67, 117.37 (d, *J*_{CF} = 23.0 Hz), 113.01 (d, *J*_{CF} = 9.3 Hz), 108.97, 101.28, 56.27, 53.23, 39.26, 38.07, 33.66; HRMS (ESI) *m/z* calcd for C₂₇H₂₅FN₃O₃ [M – H][–] 458.1885, found 458.1886.

(S)-N-(3-Fluorophenyl)-2-(2-(5-methoxy-1H-indol-3-yl)acetamido)-N-methyl-3-phenylpropanamide (6): The synthetic method was similar to that of compound **1** except that 2-(5-methoxy-1*H*-indol-3-yl)acetic acid (100 mg, 0.49 mmol, 1 equiv.) and (*S*)-2-amino-*N*-(3-fluorophenyl)-*N*-methyl-3-phenylpropanamide (TFA salt, 228 mg, 0.59 mmol, 1.2 equiv.) were used as starting materials. Yield 59%. ¹H NMR (600 MHz, CDCl₃) δ 8.36 (s, 1H), 7.31 – 7.26 (m, 2H), 7.18 (t, *J* = 7.3 Hz, 1H), 7.12 – 7.10 (m, 2H), 7.03 – 7.00 (m, 2H), 6.90 – 6.87 (m, 2H), 6.77 – 6.73 (m, 3H), 6.28 (d, *J* = 7.9 Hz, 1H), 4.79 – 4.75 (m, 1H), 3.81 (s, 3H), 3.69 – 3.62 (m, 2H), 3.14 (s, 3H), 2.75 (dd, *J* = 13.1, 8.0 Hz, 1H), 2.61 (dd, *J* = 13.1, 6.5 Hz, 1H); ¹³C NMR (150 MHz, CDCl₃) δ 171.3, 170.9, 162.8 (d, *J*_{CF} = 249.0 Hz), 154.4, 143.8, 135.8, 131.5, 130.7 (d, *J*_{CF} = 9.0 Hz), 129.2, 128.4, 127.4, 126.9, 124.4, 123.3, 115.2 (d, *J*_{CF} = 21.0 Hz), 114.7 (d, *J*_{CF} = 22.8 Hz), 113.0, 112.2, 108.3, 100.1, 55.8, 51.4, 39.2, 37.5, 33.4; HRMS (ESI) *m/z* calcd for C₂₇H₂₅FN₃O₃ [M – H][–] 458.1885, found 458.1887.

(S)-N-(4-Chlorophenyl)-2-(2-(5-methoxy-1H-indol-3-yl)acetamido)-N-methyl-3-phenylpropanamide (7): The synthetic method was similar to that of compound **1** except that 2-(5-methoxy-1*H*-indol-3-yl)acetic acid (100 mg, 0.49 mmol, 1 equiv.) and (*S*)-2-amino-*N*-(4-chlorophenyl)-*N*-methyl-3-phenylpropanamide (TFA salt, 237 mg, 0.59 mmol, 1.2 equiv.) were used as starting materials. Yield 80%. ¹H NMR (600 MHz, CD₃OD) δ 7.25 – 7.22 (m, 3H), 7.17 – 7.12 (m, 3H), 7.06 (s, 1H), 6.99 (s, 1H), 6.82 – 6.75 (m, 5H), 4.57 (t, *J* = 7.4 Hz, 1H), 3.78 (s, 3H), 3.57 (s, 2H), 3.09 (s, 3H), 2.88 (dd, *J* = 13.2, 7.7 Hz, 1H), 2.67 (dd, *J* = 13.2, 7.1 Hz, 1H); ¹³C NMR (100 MHz, CD₃OD) δ 174.1, 173.0, 155.3, 142.5, 137.8, 135.0, 133.3, 130.8, 130.2, 129.5, 128.8, 127.9, 125.7, 113.0, 113.0, 109.0, 101.4, 56.3, 53.3, 39.4, 37.9, 33.7; HRMS (ESI) *m/z* calcd for C₂₇H₂₅ClN₃O₃ [M – H][–] 474.1590, found 474.1595.

(S)-2-(2-(5-Hydroxy-1H-indol-3-yl)acetamido)-N-methyl-N,3-diphenylpropanamide (8): The synthetic method was similar to that of compound **1** except that 2-(5-hydroxy-1*H*-indol-3-yl)acetic acid (100 mg, 0.52 mmol, 1 equiv.) and (*S*)-2-amino-*N*-methyl-*N*,3-diphenylpropanamide (TFA salt, 232 mg, 0.63 mmol, 1.2 equiv.) were used as starting materials. Yield 49%. ¹H NMR (600 MHz, CDCl₃) δ 8.42 (s, 1H), 7.30 – 7.27 (m, 3H), 7.13 – 7.11 (m, 2H), 7.08 – 7.06 (m, 2H), 6.90 (s, 1H), 6.86 – 6.77 (m, 4H), 6.68 (d, *J* = 7.3 Hz, 2H), 6.60 (d, *J* = 8.1 Hz, 1H), 4.79 (q, *J* = 7.3 Hz, 1H), 3.55 (s, 2H), 3.17 (s, 3H), 2.79 (dd, *J* = 13.4, 7.0 Hz, 1H), 2.59 (dd, *J* = 13.4, 7.3 Hz, 1H); ¹³C NMR (100 MHz, CDCl₃) δ 171.7,

171.6, 150.4, 142.3, 136.0, 131.4, 129.8, 129.2, 128.3, 128.2, 127.8, 127.3, 126.7, 124.7, 112.5, 112.0, 107.6, 103.0, 51.4, 38.7, 37.8, 33; HRMS (ESI) m/z calcd for $C_{26}H_{24}N_3O_3$ [$M - H$]⁻ 426.1823, found 426.1826.

(S)-2-(2-(5-Hydroxy-1H-indol-3-yl)acetamido)-N-methyl-3-phenyl-N-(p-tolyl)propanamide (9):

The synthetic method was similar to that of compound **1** except that 2-(5-hydroxy-1*H*-indol-3-yl)acetic acid (100 mg, 0.52 mmol, 1 equiv.) and (*S*)-2-amino-*N*-methyl-3-phenyl-*N*-(*p*-tolyl)propanamide (TFA salt, 241 mg, 0.63 mmol, 1.2 equiv.) were used as starting materials. Yield 80%. ¹H NMR (600 MHz, CDCl₃) δ 8.27 (s, 1H), 7.26 (s, 1H), 7.16 – 7.08 (m, 6H), 6.91 (s, 1H), 6.79 – 6.78 (m, 3H), 6.72 (d, $J = 7.1$ Hz, 2H), 6.53 (d, $J = 8.2$ Hz, 1H), 6.27 (s, 1H), 4.83 – 4.79 (m, 1H), 3.57 (s, 2H), 3.15 (s, 3H), 2.80 (dd, $J = 13.4, 6.9$ Hz, 1H), 2.60 (dd, $J = 13.4, 7.2$ Hz, 1H), 2.33 (s, 3H); ¹³C NMR (150 MHz, CDCl₃) δ 171.7, 171.3, 150.2, 139.7, 138.2, 136.1, 131.4, 130.3, 129.2, 128.3, 127.8, 127.0, 126.7, 124.6, 112.5, 112.0, 107.8, 103.1, 51.2, 38.7, 37.8, 33.2, 21.1; HRMS (ESI) m/z calcd for $C_{27}H_{26}N_3O_3$ [$M - H$]⁻ 440.1980, found 440.1984.

(S)-N-(4-Fluorophenyl)-2-(2-(5-hydroxy-1H-indol-3-yl)acetamido)-N-methyl-3-phenylpropanamide (10):

The synthetic method was similar to that of compound **1** except that 2-(5-hydroxy-1*H*-indol-3-yl)acetic acid (100 mg, 0.52 mmol, 1 equiv.) and (*S*)-2-amino-*N*-(4-fluorophenyl)-*N*-methyl-3-phenylpropanamide (TFA salt, 241 mg, 0.63 mmol, 1.2 equiv.) were used as starting materials. Yield 49%. ¹H NMR (600 MHz, CD₃OD) δ 7.19 – 7.14 (m, 5H), 7.03 – 7.00 (m, 3H), 6.86 – 6.82 (m, 4H), 6.69 (d, $J = 8.6$ Hz, 1H), 4.56 (t, $J = 7.4$ Hz, 1H), 3.54 (s, 2H), 3.11 (s, 3H), 2.88 (dd, $J = 13.2, 7.7$ Hz, 1H), 2.68 (dd, $J = 13.2, 7.1$ Hz, 1H); ¹³C NMR (150 MHz, CD₃OD) δ 174.2, 173.2, 163.4 (d, $J_{CF} = 246.9$ Hz), 151.5, 140.96, 139.94, 137.8, 133.0, 130.7 (d, $J_{CF} = 8.8$ Hz), 130.3, 129.5, 129.2, 127.9, 125.8, 117.4 (d, $J_{CF} = 23.0$ Hz), 112.8 (d, $J_{CF} = 9.7$ Hz), 108.3, 103.6, 53.2, 39.4, 38.1, 33.7; HRMS (ESI) m/z calcd for $C_{26}H_{23}FN_3O_3$ [$M - H$]⁻ 444.1729, found 444.1732.

(S)-N-(3-Fluorophenyl)-2-(2-(5-hydroxy-1H-indol-3-yl)acetamido)-N-methyl-3-phenylpropanamide (11):

The synthetic method was similar to that of compound **1** except that 2-(5-hydroxy-1*H*-indol-3-yl)acetic acid (100 mg, 0.52 mmol, 1 equiv.) and (*S*)-2-amino-*N*-(3-fluorophenyl)-*N*-methyl-3-phenylpropanamide (TFA salt, 241 mg, 0.63 mmol, 1.2 equiv.) were used as starting materials. Yield 39%. ¹H NMR (600 MHz, CDCl₃) δ 8.30 (s, 1H), 7.27 – 7.11 (m, 5H), 6.99 – 6.94 (m, 2H), 6.85 – 6.75 (m, 5H), 6.53 (d, $J = 8.0$ Hz, 1H), 6.47 (s, 1H), 6.32 (s, 1H), 4.78 – 4.74 (m, 1H), 3.59 (s, 2H), 3.12 (s, 3H), 2.78 (dd, $J = 13.2, 8.1$ Hz, 1H), 2.63 (dd, $J = 13.2, 6.6$ Hz, 1H); ¹³C NMR (150 MHz, CDCl₃) δ 171.6, 171.5, 162.7 (d, $J_{CF} = 249.4$ Hz), 150.4, 143.6, 135.8, 131.4, 130.8 (d, $J_{CF} = 9.5$ Hz), 129.2, 128.4, 127.7, 126.9, 124.6, 123.3, 115.3 (d, $J_{CF} = 21.2$ Hz), 114.6 (d, $J_{CF} = 20.9$ Hz), 112.6, 112.1, 107.7, 103.0, 51.5, 39.0, 37.6, 33.2; HRMS (ESI) m/z calcd for $C_{26}H_{23}FN_3O_3$ [$M - H$]⁻ 444.1729, found 444.1730.

(S)-N-(4-Chlorophenyl)-2-(2-(5-hydroxy-1H-indol-3-yl)acetamido)-N-methyl-3-phenylpropanamide (12):

The synthetic method was similar to that of compound **1** except that 2-(5-hydroxy-1*H*-indol-3-yl)acetic acid (100 mg, 0.52 mmol, 1 equiv.) and (*S*)-2-amino-*N*-(4-chlorophenyl)-*N*-methyl-3-phenylpropanamide (TFA salt, 254 mg, 0.63 mmol, 1.2

equiv.) were used as starting materials. Yield 60%. ^1H NMR (600 MHz, CDCl_3) δ 8.16 (s, 1H), 7.25 – 7.12 (m, 6H), 7.00 (s, 1H), 6.82 – 6.71 (m, 5H), 6.50 (d, J = 8.0 Hz, 1H), 6.05 (s, 1H), 4.74 – 4.70 (m, 1H), 3.60 (s, 2H), 3.12 (s, 3H), 2.79 (dd, J = 13.2, 8.0 Hz, 1H), 2.62 (dd, J = 13.2, 6.7 Hz, 1H); ^{13}C NMR (150 MHz, CDCl_3) δ 171.5, 171.4, 150.3, 140.8, 135.9, 134.0, 131.3, 129.8, 129.3, 128.7, 128.4, 127.7, 126.9, 124.6, 112.6, 112.0, 107.8, 103.0, 51.3, 38.9, 37.7, 33.2; HRMS (ESI) m/z calcd for $\text{C}_{26}\text{H}_{23}\text{ClN}_3\text{O}_3$ [$\text{M} - \text{H}$] $^-$ 460.1433, found 460.1436.

(S)-N-(3-Chlorophenyl)-2-(2-(5-hydroxy-1H-indol-3-yl)acetamido)-N-methyl-3-phenylpropanamide (13). The synthetic method was similar to that of compound **1** except that 2-(5-hydroxy-1*H*-indol-3-yl)acetic acid (100 mg, 0.52 mmol, 1 equiv.) and (*S*)-2-amino-*N*-(3-chlorophenyl)-*N*-methyl-3-phenylpropanamide (TFA salt, 254 mg, 0.63 mmol, 1.2 equiv.) were used as starting materials. Yield 40%. ^1H NMR (600 MHz, CD_3OD) δ 7.23 (d, J = 8.1 Hz, 1H), 7.18 (t, J = 7.9 Hz, 1H), 7.12 – 7.06 (m, 5H), 6.96 (s, 1H), 6.77 – 6.74 (m, 4H), 6.60 (d, J = 8.6 Hz, 1H), 4.47 (t, J = 7.4 Hz, 1H), 3.49 – 3.43 (m, 2H), 3.02 (s, 3H), 2.78 (dd, J = 13.1, 8.1 Hz, 1H), 2.60 (dd, J = 13.1, 6.7 Hz, 1H); ^{13}C NMR (150 MHz, CD_3OD) δ 174.2, 173.0, 151.5, 145.1, 137.6, 135.9, 133.1, 131.9, 130.2, 129.6, 129.5, 129.2, 128.7, 128.1, 127.2, 125.8, 112.8, 112.8, 108.3, 103.6, 53.4, 39.5, 37.9, 33.7; HRMS (ESI) m/z calcd for $\text{C}_{26}\text{H}_{23}\text{ClN}_3\text{O}_3$ [$\text{M} - \text{H}$] $^-$ 460.1433, found 460.1430.

(S)-N-(3-Bromophenyl)-2-(2-(5-hydroxy-1H-indol-3-yl)acetamido)-N-methyl-3-phenylpropanamide (14). The synthetic method was similar to that of compound **1** except that 2-(5-hydroxy-1*H*-indol-3-yl)acetic acid (100 mg, 0.52 mmol, 1 equiv.) and (*S*)-2-amino-*N*-(3-bromophenyl)-*N*-methyl-3-phenylpropanamide (TFA salt, 282 mg, 0.63 mmol, 1.2 equiv.) were used as starting materials. Yield 65%. ^1H NMR (600 MHz, CD_3OD) δ 7.47 (d, J = 8.0 Hz, 1H), 7.22 – 7.17 (m, 6H), 7.06 (s, 1H), 6.87 – 6.83 (m, 4H), 6.69 (d, J = 8.6 Hz, 1H), 4.57 (t, J = 7.4 Hz, 1H), 3.59 – 3.53 (m, 2H), 3.10 (s, 3H), 2.87 (dd, J = 13.0, 8.2 Hz, 1H), 2.70 (dd, J = 13.1, 6.7 Hz, 1H); ^{13}C NMR (150 MHz, CD_3OD) δ 174.2, 173.0, 151.5, 145.2, 137.6, 133.0, 132.4, 132.1, 131.5, 130.2, 129.6, 129.2, 128.1, 127.7, 125.8, 123.6, 112.8, 112.8, 108.3, 103.6, 53.4, 39.5, 38.0, 33.7; HRMS (ESI) m/z calcd for $\text{C}_{26}\text{H}_{23}\text{BrN}_3\text{O}_3$ [$\text{M} - \text{H}$] $^-$ 504.0928, found 504.0930.

(S)-2-(2-(5-Hydroxy-1H-indol-3-yl)acetamido)-N-methyl-3-phenyl-N-(3-(trifluoromethyl)phenyl)propanamide (15). The synthetic method was similar to that of compound **1** except that 2-(5-hydroxy-1*H*-indol-3-yl)acetic acid (100 mg, 0.52 mmol, 1 equiv.) and (*S*)-2-amino-*N*-methyl-3-phenyl-*N*-(3-(trifluoromethyl)phenyl)propanamide (TFA salt, 275 mg, 0.63 mmol, 1.2 equiv.) were used as starting materials. Yield 49%. ^1H NMR (600 MHz, CD_3OD) δ 7.60 (d, J = 7.7 Hz, 1H), 7.47 (t, J = 7.8 Hz, 1H), 7.18 – 7.12 (m, 6H), 7.04 (s, 1H), 6.86 (s, 1H), 6.81 (d, J = 7.2 Hz, 2H), 6.68 (d, J = 8.6 Hz, 1H), 4.52 (t, J = 7.4 Hz, 1H), 3.58 – 3.52 (m, 2H), 3.13 (s, 3H), 2.87 (dd, J = 12.9, 8.3 Hz, 1H), 2.68 (dd, J = 13.0, 6.7 Hz, 1H); ^{13}C NMR (150 MHz, CD_3OD) δ 174.2, 173.1, 151.4, 144.6, 137.6, 133.0, 132.7, 131.8, 130.1, 129.6, 129.10, 129.09, 128.0, 126.0, 125.7, 125.4, 124.9 (q, J_{CF} = 271.2 Hz), 112.8, 112.8, 112.7, 108.3, 53.4, 39.5, 38.0, 33.7; HRMS (ESI) m/z calcd for $\text{C}_{27}\text{H}_{23}\text{F}_3\text{N}_3\text{O}_3$ [$\text{M} - \text{H}$] $^-$ 494.1697, found 494.1693.

(2S)-N-Methyl-2-(2-(7-methyl-2-oxoindolin-3-yl)acetamido)-N,3-diphenylpropanamide

(16): The synthetic method was similar to that of compound **1** except that 2-(7-methyl-2-oxoindolin-3-yl)acetic acid (100 mg, 0.49 mmol, 1 equiv.) and (*S*)-2-amino-*N*-methyl-*N*,3-diphenylpropanamide (TFA salt, 215 mg, 0.58 mmol, 1.2 equiv.) were used as starting materials. (Yield 70%, dr 1.1:1). ¹H NMR (600 MHz, CD₃OD) δ 7.36 – 7.31 (m, 3H), 7.22 – 7.17 (m, 3H), 6.99 – 6.95 (m, 2H), 6.88 – 6.83 (m, 3H), 6.75 (t, *J* = 7.6 Hz, 1H), 6.65 (d, *J* = 7.4 Hz, 1H), 4.73 – 4.63 (m, 1H), 3.72 – 3.69 (m, 1H), 3.18 – 3.15 (m, 1H), 2.96 – 2.82 (m, 2H), 2.71 – 2.65 (m, 1H), 2.54 – 2.47 (m, 1H), 2.22 (s, 3H); ¹³C NMR (100 MHz, CD₃OD) δ 181.8, 181.7, 173.1, 172.3, 172.0, 144.0, 143.9, 142.0, 141.9, 138.2, 138.1, 130.8, 130.5, 130.4, 130.3, 130.2, 130.0, 129.5, 129.3, 128.6, 127.9, 127.8, 123.3, 123.3, 122.9, 122.6, 120.5, 120.4, 53.5, 53.1, 39.5, 39.4, 38.1, 38.0, 37.1, 37.0, 16.7; HRMS (ESI) *m/z* calcd for C₂₇H₂₆N₃O₃ [M – H][–] 440.1980, found 440.1985.

(2S)-N-(4-Chlorophenyl)-N-methyl-2-(2-(7-methyl-2-oxoindolin-3-yl)acetamido)-3-phenylpropanamide (17):

The synthetic method was similar to that of compound **1** except that 2-(7-methyl-2-oxoindolin-3-yl)acetic acid (100 mg, 0.49 mmol, 1 equiv.) and (*S*)-2-amino-*N*-(4-chlorophenyl)-*N*-methyl-3-phenylpropanamide (TFA salt, 238 mg, 0.59 mmol, 1.2 equiv.) were used as starting materials. (Yield 70%, dr 1.1:1). ¹H NMR (600 MHz, CD₃OD) δ 7.30 – 7.21 (m, 5H), 6.99 – 6.86 (m, 4H), 6.81 – 6.75 (m, 2H), 6.62 (s, 1H), 4.63 – 4.55 (m, 1H), 3.73 – 3.68 (m, 1H), 3.13 – 3.08 (m, 3H), 2.96 – 2.82 (m, 2H), 2.71 – 2.53 (m, 2H), 2.23 – 2.22 (m, 3H); ¹³C NMR (100 MHz, CD₃OD) δ 181.8, 181.7, 173.1, 173.0, 172.2, 171.9, 142.6, 142.5, 142.2, 142.0, 138.02, 134.92, 130.72, 130.50, 130.4, 130.3, 130.28, 130.19, 130.1, 130.0, 129.60, 128.0, 123.32, 122.8, 122.6, 120.5, 53.4, 52.9, 44.3, 44.2, 39.71, 39.5, 38.0, 37.8, 37.1, 36.9, 16.7; HRMS (ESI) *m/z* calcd for C₂₇H₂₅ClN₃O₃ [M – H][–] 474.1590, found 474.1595.

(2S)-N-(3-Chlorophenyl)-N-methyl-2-(2-(7-methyl-2-oxoindolin-3-yl)acetamido)-3-phenylpropanamide (18):

The synthetic method was similar to that of compound **1** except that 2-(7-methyl-2-oxoindolin-3-yl)acetic acid (100 mg, 0.49 mmol, 1 equiv.) and (*S*)-2-amino-*N*-(3-chlorophenyl)-*N*-methyl-3-phenylpropanamide (TFA salt, 238 mg, 0.59 mmol, 1.2 equiv.) were used as starting materials. (Yield 72%, dr 1:1). ¹H NMR (600 MHz, CD₃OD) δ 7.31 – 7.24 (m, 6H), 7.01 – 6.88 (m, 5H), 6.81 – 6.77 (m, 1H), 6.67 (s, 1H), 4.62 – 4.55 (m, 1H), 3.76 – 3.71 (m, 1H), 3.13 – 3.09 (m, 3H), 2.96 – 2.84 (m, 2H), 2.73 – 2.69 (m, 1H), 2.55 – 2.51 (m, 1H), 2.23 (s, 3H); ¹³C NMR (100 MHz, CD₃OD) δ 181.75, 173.0, 172.9, 172.3, 172.0, 145.2, 145.0, 142.1, 142.0, 137.9, 135.9, 131.8, 130.5, 130.3, 130.1, 130.0, 129.7, 129.6, 129.4, 128.8, 128.1, 127.24, 123.4, 123.3, 122.9, 122.7, 122.6, 120.5, 53.6, 53.1, 44.3, 39.8, 39.7, 38.0, 37.8, 37.1, 36.9, 16.7; HRMS (ESI) *m/z* calcd for C₂₇H₂₅ClN₃O₃ [M – H][–] 474.1590, found 474.1594.

(2S)-N-(3-Fluorophenyl)-N-methyl-2-(2-(7-methyl-2-oxoindolin-3-yl)acetamido)-3-phenylpropanamide (19):

The synthetic method was similar to that of compound **1** except that 2-(7-methyl-2-oxoindolin-3-yl)acetic acid (100 mg, 0.49 mmol, 1 equiv.) and (*S*)-2-amino-*N*-(3-fluorophenyl)-*N*-methyl-3-phenylpropanamide (TFA salt, 227 mg, 0.59 mmol, 1.2 equiv.) were used as starting materials. (Yield 69%, dr 1:1). ¹H NMR (600 MHz, CD₃OD) δ 7.34 – 7.22 (m, 4H), 7.08 – 7.05 (m, 1H), 7.00 – 6.87 (m, 5H), 6.79 – 6.73 (m,

2H), 6.57 (s, 1H), 4.67 – 4.59 (m, 1H), 3.75 – 3.70 (m, 1H), 3.15 – 3.11 (m, 3H), 2.97 – 2.82 (m, 2H), 2.73 – 2.68 (m, 1H), 2.55 – 2.50 (m, 1H), 2.22 (s, 3H); HRMS (ESI) m/z calcd for $C_{27}H_{25}FN_3O_3$ $[M - H]^-$ 458.1885, found 458.1890.

(2S)-2-(2-(4,7-Dimethyl-2-oxoindolin-3-yl)acetamido)-N-methyl-N,3-

diphenylpropanamide (20).: The synthetic method was similar to that of compound **1** except that 2-(4,7-dimethyl-2-oxoindolin-3-yl)acetic acid (100 mg, 0.46 mmol, 1 equiv.) and (*S*)-2-amino-*N*-methyl-*N*,3-diphenylpropanamide (TFA salt, 203 mg, 0.55 mmol, 1.2 equiv.) were used as starting materials. (Yield 58%, dr 1.2:1). 1H NMR (600 MHz, CD_3OD) δ 7.30 – 7.24 (m, 2H), 7.20 – 7.14 (m, 4H), 6.92 – 6.82 (m, 3H), 6.69 – 6.62 (m, 1H), 6.45 (s, 1H), 4.58 – 4.52 (m, 1H), 3.68 – 3.67 (m, 1H), 3.14 – 3.06 (m, 3H), 3.01 – 2.81 (m, 3H), 2.65 – 2.59 (m, 1H), 2.23 – 2.16 (m, 6H); ^{13}C NMR (100 MHz, CD_3OD) δ 182.1, 182.0, 173.1, 172.9, 171.8, 171.3, 143.9, 143.6, 142.5, 142.2, 138.1, 133.1, 132.8, 130.8, 130.6, 130.5, 130.4, 130.3, 130.2, 129.4, 129.2, 129.1, 128.5, 127.8, 125.0, 124.9, 117.9, 117.8, 53.1, 52.6, 39.8, 39.5, 38.0, 37.8, 36.1, 36.0, 18.6, 16.4; HRMS (ESI) m/z calcd for $C_{28}H_{28}N_3O_3$ $[M - H]^-$ 454.2136, found 454.2145.

(2S)-2-(2-(4,7-Dimethyl-2-oxoindolin-3-yl)acetamido)-N-(4-fluorophenyl)-N-methyl-3-

phenylpropanamide (21).: The synthetic method was similar to that of compound **1** except that 2-(4,7-dimethyl-2-oxoindolin-3-yl)acetic acid (100 mg, 0.46 mmol, 1 equiv.) and (*S*)-2-amino-*N*-(4-fluorophenyl)-*N*-methyl-3-phenylpropanamide (TFA salt, 212 mg, 0.55 mmol, 1.2 equiv.) were used as starting materials. (Yield 65%, dr 1.1:1). 1H NMR (600 MHz, CD_3OD) δ 8.27 – 8.14 (m, 1H), 7.31 – 7.18 (m, 3H), 6.99 – 6.82 (m, 6H), 6.70 – 6.64 (m, 1H), 6.31 (s, 1H), 4.53 – 4.46 (m, 1H), 3.69 – 3.65 (m, 1H), 3.10 – 3.01 (m, 3H), 2.99 – 2.85 (m, 3H), 2.65 – 2.61 (m, 1H), 2.23 – 2.17 (m, 6H); HRMS (ESI) m/z calcd for $C_{28}H_{27}FN_3O_3$ $[M - H]^-$ 472.2042, found 472.2047.

(2S)-2-(2-(4,7-Dimethyl-2-oxoindolin-3-yl)acetamido)-N-(3-fluorophenyl)-N-methyl-3-

phenylpropanamide (22).: The synthetic method was similar to that of compound **1** except that 2-(4,7-dimethyl-2-oxoindolin-3-yl)acetic acid (100 mg, 0.46 mmol, 1 equiv.) and (*S*)-2-amino-*N*-(3-fluorophenyl)-*N*-methyl-3-phenylpropanamide (TFA salt, 212 mg, 0.55 mmol, 1.2 equiv.) were used as starting materials. (Yield 68%, dr 1:1). 1H NMR (600 MHz, CD_3OD) δ 7.28 – 7.11 (m, 4H), 7.05 – 6.86 (m, 4H), 6.69 – 6.41 (m, 2H), 6.19 – 6.04 (m, 1H), 4.56 – 4.50 (m, 1H), 3.70 – 3.65 (m, 1H), 3.11 – 3.02 (m, 3H), 3.00 – 2.85 (m, 3H), 2.67 – 2.64 (m, 1H), 2.21 – 2.17 (m, 6H); HRMS (ESI) m/z calcd for $C_{28}H_{27}FN_3O_3$ $[M - H]^-$ 472.2042, found 472.2046.

(2S)-N-(4-Chlorophenyl)-2-(2-(4,7-dimethyl-2-oxoindolin-3-yl)acetamido)-N-methyl-3-

phenylpropanamide (23).: The synthetic method was similar to that of compound **1** except that 2-(4,7-dimethyl-2-oxoindolin-3-yl)acetic acid (100 mg, 0.46 mmol, 1 equiv.) and (*S*)-2-amino-*N*-(4-chlorophenyl)-*N*-methyl-3-phenylpropanamide (TFA salt, 222 mg, 0.55 mmol, 1.2 equiv.) were used as starting materials. (Yield 72%, dr 1:1). 1H NMR (600 MHz, CD_3OD) δ 7.24 – 7.18 (m, 4H), 7.08 (d, $J = 8.6$ Hz, 1H), 6.92 – 6.85 (m, 3H), 6.70 – 6.63 (m, 2H), 6.23 (s, 1H), 4.51 – 4.45 (m, 1H), 3.68 – 3.63 (m, 1H), 3.09 – 2.99 (m, 3H), 2.91 – 2.84 (m, 3H), 2.65 – 2.60 (m, 1H), 2.23 – 2.16 (m, 6H); ^{13}C NMR (100 MHz, CD_3OD) δ

182.1, 181.9, 173.0, 172.7, 171.8, 171.1, 142.7, 142.5, 142.2, 138.0, 134.9, 134.7, 133.0, 132.8, 130.7, 130.6, 130.5, 130.4, 130.3, 130.1, 129.5, 127.9, 127.8, 127.7, 125.0, 124.9, 117.9, 117.8, 53.0, 52.4, 44.2, 44.1, 39.9, 39.6, 37.9, 37.6, 36.0, 18.6, 16.4; HRMS (ESI) m/z calcd for $C_{28}H_{27}ClN_3O_3$ $[M - H]^-$ 488.1746, found 488.1750.

(2S)-N-(3-Chlorophenyl)-2-(2-(4,7-dimethyl-2-oxoindolin-3-yl)acetamido)-N-methyl-3-phenylpropanamide (24).: The synthetic method was similar to that of compound **1** except that 2-(4,7-dimethyl-2-oxoindolin-3-yl)acetic acid (100 mg, 0.46 mmol, 1 equiv.) and (*S*)-2-amino-*N*-(3-chlorophenyl)-*N*-methyl-3-phenylpropanamide (TFA salt, 222 mg, 0.55 mmol, 1.2 equiv.) were used as starting materials. (Yield 79%, dr 1:1). 1H NMR (600 MHz, CD_3OD) δ 7.27 – 7.07 (m, 6H), 6.91 – 6.85 (m, 3H), 6.68 – 6.63 (m, 1H), 6.29 (s, 1H), 4.51 – 4.46 (m, 1H), 3.70 – 3.65 (m, 1H), 3.07 – 2.99 (m, 3H), 2.96 – 2.84 (m, 3H), 2.66 – 2.63 (m, 1H), 2.21 – 2.16 (m, 6H); ^{13}C NMR (100 MHz, CD_3OD) δ 182.0, 181.9, 172.9, 172.7, 171.8, 171.3, 145.0, 144.7, 142.5, 142.1, 137.9, 137.8, 135.8, 135.6, 133.0, 132.8, 131.8, 131.6, 130.5, 130.3, 129.6, 129.3, 128.6, 128.0, 127.8, 127.2, 127.1, 125.0, 124.9, 117.9, 117.8, 53.1, 52.6, 44.2, 39.8, 37.9, 37.7, 36.1, 18.6, 16.5; HRMS (ESI) m/z calcd for $C_{28}H_{27}ClN_3O_3$ $[M - H]^-$ 488.1746, found 488.1751.

(S)-N-Methyl-2-(2-(naphthalen-2-yl)acetamido)-N,3-diphenylpropanamide (25).: The synthetic method was similar to that of compound **1** except that 2-(naphthalen-2-yl)acetic acid (100 mg, 0.54 mmol, 1 equiv.) and (*S*)-2-amino-*N*-methyl-*N*,3-diphenylpropanamide (TFA salt, 239 mg, 0.65 mmol, 1.2 equiv.) were used as starting materials. Yield 79%. 1H NMR (600 MHz, CD_3OD) δ 8.26 (d, $J = 7.5$ Hz, 1H), 7.81 – 7.74 (m, 3H), 7.64 (s, 1H), 7.46 – 7.42 (m, 2H), 7.35 – 7.34 (m, 3H), 7.28 – 7.27 (m, 1H), 7.15 – 7.03 (m, 4H), 6.81 (d, $J = 7.2$ Hz, 2H), 4.69 – 4.65 (m, 1H), 3.66 – 3.61 (m, 2H), 3.19 (s, 3H), 2.95 (dd, $J = 13.4$, 6.4 Hz, 1H), 2.72 (dd, $J = 13.4$, 8.4 Hz, 1H); ^{13}C NMR (150 MHz, CD_3OD) δ 173.4, 173.3, 144.0, 138.1, 135.0, 134.2, 133.9, 130.9, 130.1, 129.4, 129.4, 129.1, 128.8, 128.7, 128.6, 128.6, 128.3, 127.8, 127.1, 126.7, 53.6, 43.5, 39.0, 38.1; HRMS (ESI) m/z calcd for $C_{28}H_{25}N_2O_2$ $[M - H]^-$ 421.1922, found 421.1927.

(S)-N-Methyl-2-(2-(naphthalen-2-yl)acetamido)-3-phenyl-N-(p-tolyl)propanamide (26).: The synthetic method was similar to that of compound **1** except that 2-(naphthalen-2-yl)acetic acid (100 mg, 0.54 mmol, 1 equiv.) and (*S*)-2-amino-*N*-methyl-3-phenyl-*N*-(*p*-tolyl)propanamide (TFA salt, 249 mg, 0.65 mmol, 1.2 equiv.) were used as starting materials. Yield 58%. 1H NMR (600 MHz, $CDCl_3$) δ 7.83 – 7.77 (m, 3H), 7.63 (s, 1H), 7.49 – 7.45 (m, 2H), 7.28 – 7.26 (m, 1H), 7.14 – 7.05 (m, 5H), 6.79 – 6.75 (m, 4H), 6.17 (d, $J = 8.2$ Hz, 1H), 4.84 – 4.80 (m, 1H), 3.67 – 3.62 (m, 2H), 3.17 (s, 3H), 2.81 (dd, $J = 13.4$, 6.9 Hz, 1H), 2.62 (dd, $J = 13.4$, 7.1 Hz, 1H), 2.35 (s, 3H); ^{13}C NMR (100 MHz, $CDCl_3$) δ 171.4, 170.0, 139.9, 138.1, 136.1, 133.6, 132.5, 132.2, 130.4, 129.2, 128.6, 128.3, 128.1, 127.7, 127.7, 127.3, 127.0, 126.7, 126.2, 125.9, 51.0, 43.8, 38.8, 37.7, 21.1; HRMS (ESI) m/z calcd for $C_{29}H_{27}N_2O_2$ $[M - H]^-$ 435.2079, found 435.2083.

(S)-N-(4-Chlorophenyl)-N-methyl-2-(2-(naphthalen-2-yl)acetamido)-3-phenylpropanamide (27).: The synthetic method was similar to that of compound **1** except that 2-(naphthalen-2-yl)acetic acid (100 mg, 0.54 mmol, 1 equiv.) and (*S*)-2-amino-*N*-(4-

chlorophenyl)-*N*-methyl-3-phenylpropanamide (TFA salt, 262 mg, 0.65 mmol, 1.2 equiv.) were used as starting materials. Yield 70%. ¹H NMR (600 MHz, CD₃OD) δ 7.80 – 7.74 (m, 3H), 7.65 (s, 1H), 7.45 – 7.41 (m, 2H), 7.30 – 7.26 (m, 3H), 7.18 – 7.13 (m, 3H), 6.88 – 6.87 (m, 4H), 4.59 (t, *J* = 7.5 Hz, 1H), 3.65 – 3.61 (m, 2H), 3.12 (s, 3H), 2.95 (dd, *J* = 13.3, 7.5 Hz, 1H), 2.74 (dd, *J* = 13.3, 7.5 Hz, 1H); ¹³C NMR (100 MHz, CD₃OD) δ 173.3, 173.2, 142.6, 137.9, 135.0, 134.2, 133.9, 130.8, 130.3, 129.5, 129.1, 128.8, 128.7, 128.6, 128.3, 128.0, 127.1, 126.7, 53.5, 43.4, 39.2, 38.0; HRMS (ESI) *m/z* calcd for C₂₈H₂₄ClN₂O₂ [M – H][–] 455.1532, found 455.1531.

(S)-N-(3-Chlorophenyl)-N-methyl-2-(2-(naphthalen-2-yl)acetamido)-3-

phenylpropanamide (28).: The synthetic method was similar to that of compound **1** except that 2-(naphthalen-2-yl)acetic acid (100 mg, 0.54 mmol, 1 equiv.) and (*S*)-2-amino-*N*-(3-chlorophenyl)-*N*-methyl-3-phenylpropanamide (TFA salt, 262 mg, 0.65 mmol, 1.2 equiv.) were used as starting materials. Yield 90%. ¹H NMR (600 MHz, CD₃OD) δ 7.79 – 7.74 (m, 3H), 7.67 (s, 1H), 7.44 – 7.40 (m, 2H), 7.32 – 7.24 (m, 3H), 7.19 – 7.13 (m, 3H), 6.93 – 6.76 (m, 4H), 4.58 (t, *J* = 7.4 Hz, 1H), 3.64 (s, 2H), 3.11 (s, 3H), 2.95 (dd, *J* = 13.1, 7.9 Hz, 1H), 2.75 (dd, *J* = 13.1, 7.3 Hz, 1H); ¹³C NMR (100 MHz, CD₃OD) δ 173.4, 173.1, 145.1, 137.8, 135.9, 135.0, 134.2, 133.9, 131.9, 130.2, 129.6, 129.4, 129.1, 128.8, 128.7, 128.7, 128.6, 128.3, 128.1, 127.2, 127.1, 126.7, 53.6, 43.4, 39.4, 38.0; HRMS (ESI) *m/z* calcd for C₂₈H₂₄ClN₂O₂ [M – H][–] 455.1532, found 455.1533.

(S)-N-(3-Fluorophenyl)-N-methyl-2-(2-(naphthalen-2-yl)acetamido)-3-

phenylpropanamide (29).: The synthetic method was similar to that of compound **1** except that 2-(naphthalen-2-yl)acetic acid (100 mg, 0.54 mmol, 1 equiv.) and (*S*)-2-amino-*N*-(3-fluorophenyl)-*N*-methyl-3-phenylpropanamide (TFA salt, 251 mg, 0.65 mmol, 1.2 equiv.) were used as starting materials. Yield 79%. ¹H NMR (600 MHz, CD₃OD) δ 7.79 – 7.73 (m, 3H), 7.66 (s, 1H), 7.44 – 7.40 (m, 2H), 7.31 – 7.27 (m, 2H), 7.17 – 7.11 (m, 3H), 7.06 (t, *J* = 7.9 Hz, 1H), 6.87 – 6.81 (m, 3H), 6.62 (s, 1H), 4.63 (t, *J* = 7.4 Hz, 1H), 3.66 – 3.61 (m, 2H), 3.13 (s, 3H), 2.95 (dd, *J* = 13.2, 7.5 Hz, 1H), 2.74 (dd, *J* = 13.2, 7.6 Hz, 1H); ¹³C NMR (100 MHz, CD₃OD) δ 173.4, 173.2, 164.2 (d, *J*_{CF} = 247.4 Hz), 145.4 (d, *J*_{CF} = 9.7 Hz), 137.9, 135.0, 134.2, 133.9, 132.1 (d, *J*_{CF} = 9.1 Hz), 130.2, 129.5, 129.1, 128.8, 128.7, 128.6, 128.3, 128.0, 127.1, 126.7, 124.7, 116.2 (d, *J*_{CF} = 21.3 Hz), 115.9 (d, *J*_{CF} = 23.1 Hz), 53.6, 43.4, 39.3, 38.0; HRMS (ESI) *m/z* calcd for C₂₈H₂₄FN₂O₂ [M – H][–] 439.1827, found 439.1830.

(S)-N-Ethyl-2-(2-(naphthalen-2-yl)acetamido)-N,3-diphenylpropanamide (30).: The synthetic method was similar to that of compound **1** except that 2-(naphthalen-2-yl)acetic acid (100 mg, 0.54 mmol, 1 equiv.) and (*S*)-2-amino-*N*-ethyl-*N*,3-diphenylpropanamide (TFA salt, 249 mg, 0.65 mmol, 1.2 equiv.) were used as starting materials. Yield 80%. ¹H NMR (600 MHz, CDCl₃) δ 7.83 – 7.78 (m, 3H), 7.64 (s, 1H), 7.50 – 7.45 (m, 2H), 7.36 – 7.34 (m, 3H), 7.27 – 7.26 (m, 1H), 7.14 (t, *J* = 7.4 Hz, 1H), 7.06 (t, *J* = 7.6 Hz, 2H), 6.91 – 6.86 (m, 1H), 6.73 (d, *J* = 7.3 Hz, 2H), 6.08 (d, *J* = 8.1 Hz, 1H), 4.72 – 4.68 (m, 1H), 3.81 – 3.75 (m, 1H), 3.67 – 3.62 (m, 2H), 3.59 – 3.53 (m, 1H), 2.82 (dd, *J* = 13.4, 6.9 Hz, 1H), 2.60 (dd, *J* = 13.4, 7.1 Hz, 1H), 1.06 (t, *J* = 7.2 Hz, 3H); ¹³C NMR (100 MHz, CDCl₃) δ 170.7, 169.9, 140.8, 136.1, 133.6, 132.5, 132.2, 129.7, 129.3, 128.6, 128.4, 128.3, 128.1, 127.7,

127.7, 127.3, 126.8, 126.2, 125.9, 51.4, 44.6, 43.8, 38.8, 12.8; HRMS (ESI) m/z calcd for $C_{29}H_{27}N_2O_2$ [M – H][–] 435.2079, found 435.2081.

(S)-N-Methyl-2-(2-(naphthalen-1-yl)acetamido)-N,3-diphenylpropanamide (31): The synthetic method was similar to that of compound **1** except that 2-(naphthalen-1-yl)acetic acid (100 mg, 0.54 mmol, 1 equiv.) and (*S*)-2-amino-*N*-methyl-*N*,3-diphenylpropanamide (TFA salt, 239 mg, 0.65 mmol, 1.2 equiv.) were used as starting materials. Yield 70%. ¹H NMR (600 MHz, CD₃OD) δ 7.86 – 7.83 (m, 2H), 7.76 (d, J = 8.2 Hz, 1H), 7.46 – 7.42 (m, 2H), 7.39 – 7.36 (m, 1H), 7.33 – 7.29 (m, 4H), 7.17 – 7.10 (m, 3H), 7.00 (m, 2H), 6.77 (d, J = 7.3 Hz, 2H), 4.68 – 4.66 (m, 1H), 3.94 (s, 2H), 3.17 (s, 3H), 2.92 (dd, J = 13.4, 6.3 Hz, 1H), 2.70 (dd, J = 13.4, 8.4 Hz, 2H); ¹³C NMR (150 MHz, CD₃OD) δ 173.3, 173.2, 143.9, 138.0, 135.3, 133.5, 132.8, 130.8, 130.1, 129.6, 129.4, 129.3, 129.0, 128.8, 128.6, 127.8, 127.3, 126.7, 126.5, 124.9, 53.5, 40.9, 39.0, 38.1; HRMS (ESI) m/z calcd for $C_{28}H_{25}N_2O_2$ [M – H][–] 421.1922, found 421.1928.

(S)-N-Methyl-2-(2-(naphthalen-1-yl)acetamido)-3-phenyl-N-(p-tolyl)propanamide (32): The synthetic method was similar to that of compound **1** except that 2-(naphthalen-1-yl)acetic acid (100 mg, 0.54 mmol, 1 equiv.) and (*S*)-2-amino-*N*-methyl-3-phenyl-*N*-(*p*-tolyl)propanamide (TFA salt, 249 mg, 0.65 mmol, 1.2 equiv.) were used as starting materials.

Yield 69%. ¹H NMR (600 MHz, CDCl₃) δ 7.87 – 7.85 (m, 2H), 7.80 (d, J = 8.2 Hz, 1H), 7.50 – 7.41 (m, 3H), 7.35 (d, J = 6.9 Hz, 1H), 7.13 – 7.08 (m, 3H), 7.01 (t, J = 7.6 Hz, 2H), 6.75 (s, 1H), 6.60 (d, J = 7.4 Hz, 2H), 6.08 (d, J = 8.3 Hz, 1H), 4.82 – 4.78 (m, 1H), 3.99 – 3.90 (m, 2H), 3.12 (s, 3H), 2.68 (dd, J = 13.3, 6.9 Hz, 1H), 2.51 (dd, J = 13.4, 7.0 Hz, 1H), 2.35 (s, 3H); ¹³C NMR (100 MHz, CDCl₃) δ 171.2, 169.9, 139.8, 138.1, 136.0, 133.9, 132.1, 131.0, 130.4, 129.1, 128.7, 128.3, 128.2, 128.2, 127.0, 126.6, 126.5, 126.0, 125.7, 123.8, 51.0, 41.6, 38.7, 37.6, 21.1; HRMS (ESI) m/z calcd for $C_{29}H_{27}N_2O_2$ [M – H][–] 435.2079, found 435.2085.

(S)-N-(4-Chlorophenyl)-N-methyl-2-(2-(naphthalen-1-yl)acetamido)-3-phenylpropanamide (33): The synthetic method was similar to that of compound **1** except that 2-(naphthalen-1-yl)acetic acid (100 mg, 0.54 mmol, 1 equiv.) and (*S*)-2-amino-*N*-(4-chlorophenyl)-*N*-methyl-3-phenylpropanamide (TFA salt, 262 mg, 0.65 mmol, 1.2 equiv.) were used as starting materials. Yield 80%. ¹H NMR (600 MHz, CD₃OD) δ 7.90 – 7.84 (m, 2H), 7.77 (d, J = 8.2 Hz, 1H), 7.46 – 7.45 (m, 2H), 7.40 – 7.37 (m, 1H), 7.32 (d, J = 6.9 Hz, 1H), 7.25 – 7.15 (m, 5H), 6.86 – 6.85 (m, 4H), 4.59 (t, J = 7.5 Hz, 1H), 3.98 – 3.93 (m, 2H), 3.12 (s, 3H), 2.93 (dd, J = 13.3, 7.4 Hz, 1H), 2.74 (dd, J = 13.3, 7.6 Hz, 1H); ¹³C NMR (100 MHz, CD₃OD) δ 173.3, 173.2, 142.6, 138.0, 135.4, 135.0, 133.6, 132.8, 130.8, 130.3, 130.2, 129.7, 129.6, 129.1, 128.9, 128.0, 127.3, 126.8, 126.6, 124.9, 53.5, 40.8, 39.2, 38.0; HRMS (ESI) m/z calcd for $C_{28}H_{24}ClN_2O_2$ [M – H][–] 455.1532, found 455.1534.

(S)-N-(3-Chlorophenyl)-N-methyl-2-(2-(naphthalen-1-yl)acetamido)-3-phenylpropanamide (34): The synthetic method was similar to that of compound **1** except that 2-(naphthalen-1-yl)acetic acid (100 mg, 0.54 mmol, 1 equiv.) and (*S*)-2-amino-*N*-(3-chlorophenyl)-*N*-methyl-3-phenylpropanamide (TFA salt, 262 mg, 0.65 mmol, 1.2 equiv.)

were used as starting materials. Yield 82%. ^1H NMR (600 MHz, CD_3OD) δ 7.91 – 7.90 (m, 1H), 7.85 – 7.83 (m, 1H), 7.76 (d, J = 8.2 Hz, 1H), 7.47 – 7.44 (m, 2H), 7.40 – 7.16 (m, 8H), 6.91 – 6.85 (m, 3H), 4.60 – 4.57 (m, 1H), 3.99 – 3.93 (m, 2H), 3.11 (s, 3H), 2.93 (dd, J = 13.1, 7.8 Hz, 1H), 2.74 (dd, J = 13.1, 7.3 Hz, 1H); ^{13}C NMR (100 MHz, CD_3OD) δ 173.3, 173.1, 145.1, 137.8, 135.9, 135.3, 133.6, 132.8, 131.9, 130.2, 129.7, 129.6, 129.4, 129.0, 128.9, 128.7, 128.1, 127.3, 127.2, 126.8, 126.6, 124.9, 53.6, 40.8, 39.3, 38.0; HRMS (ESI) m/z calcd for $\text{C}_{28}\text{H}_{24}\text{ClN}_2\text{O}_2$ $[\text{M} - \text{H}]^-$ 455.1532, found 455.1535.

(S)-N-(3-Fluorophenyl)-N-methyl-2-(2-(naphthalen-1-yl)acetamido)-3-phenylpropanamide (35):

The synthetic method was similar to that of compound **1** except that 2-(naphthalen-1-yl)acetic acid (100 mg, 0.54 mmol, 1 equiv.) and (*S*)-2-amino-*N*-(3-fluorophenyl)-*N*-methyl-3-phenylpropanamide (TFA salt, 251 mg, 0.65 mmol, 1.2 equiv.) were used as starting materials. Yield 65%. ^1H NMR (600 MHz, CD_3OD) δ 8.23 (d, J = 6.7 Hz, 1H), 7.90 – 7.76 (m, 3H), 7.46 – 7.26 (m, 6H), 7.20 – 7.14 (m, 3H), 7.05 (t, J = 7.8 Hz, 1H), 6.85 – 6.80 (m, 3H), 6.61 (s, 1H), 4.66 – 4.63 (m, 1H), 3.96 (s, 2H), 3.13 (s, 3H), 2.94 (dd, J = 13.2, 7.3 Hz, 1H), 2.74 (dd, J = 13.1, 7.7 Hz, 1H); ^{13}C NMR (100 MHz, CD_3OD) δ 173.4, 173.1, 164.2 (d, J = 247.5 Hz), 145.4 (d, J = 9.5 Hz), 137.9, 135.3, 133.6, 132.7, 132.1 (d, J = 9.2 Hz), 130.2, 129.7, 129.5, 129.0, 128.8, 128.0, 127.3, 126.8, 126.5, 124.9, 124.7, 116.2 (d, J = 21.1 Hz), 115.9 (d, J = 22.7 Hz), 53.5, 40.8, 39.2, 37.9; HRMS (ESI) m/z calcd for $\text{C}_{28}\text{H}_{24}\text{FN}_2\text{O}_2$ $[\text{M} - \text{H}]^-$ 439.1827, found 439.1831.

(S)-N-Ethyl-2-(2-(naphthalen-1-yl)acetamido)-N,3-diphenylpropanamide (36): The synthetic method was similar to that of compound **1** except that 2-(naphthalen-1-yl)acetic acid (100 mg, 0.54 mmol, 1 equiv.) and (*S*)-2-amino-*N*-ethyl-*N*,3-diphenylpropanamide (TFA salt, 249 mg, 0.65 mmol, 1.2 equiv.) were used as starting materials. Yield 69%. ^1H NMR (600 MHz, CDCl_3) δ 7.87 – 7.85 (m, 2H), 7.80 (d, J = 8.2 Hz, 1H), 7.50 – 7.41 (m, 3H), 7.36 – 7.32 (m, 4H), 7.09 (t, J = 7.4 Hz, 1H), 7.02 – 6.99 (m, 2H), 6.83 (s, 1H), 6.60 (d, J = 7.4 Hz, 2H), 6.07 (d, J = 8.3 Hz, 1H), 4.70 – 4.66 (m, 1H), 3.99 – 3.90 (m, 2H), 3.74 – 3.71 (m, 1H), 3.53 – 3.47 (m, 1H), 2.69 (dd, J = 13.3, 6.9 Hz, 1H), 2.50 (dd, J = 13.3, 7.0 Hz, 1H), 1.01 (t, J = 7.2 Hz, 3H); ^{13}C NMR (100 MHz, CDCl_3) δ 170.5, 169.9, 140.7, 136.0, 133.9, 132.1, 131.0, 129.7, 129.2, 128.7, 128.4, 128.3, 128.2, 128.2, 126.6, 126.5, 126.0, 125.7, 123.8, 51.3, 44.6, 41.6, 38.8, 12.7; HRMS (ESI) m/z calcd for $\text{C}_{29}\text{H}_{27}\text{N}_2\text{O}_2$ $[\text{M} - \text{H}]^-$ 435.2079, found 435.2083.

(S)-2-(2-(1,3-Dimethyl-2,6-dioxo-1,2,3,6-tetrahydro-7H-purin-7-yl)acetamido)-N-methyl-N,3-diphenylpropanamide (37): The synthetic method was similar to that of compound **1** except that 2-(1,3-dimethyl-2,6-dioxo-1,2,3,6-tetrahydro-7H-purin-7-yl)acetic acid (100 mg, 0.42 mmol, 1 equiv.) and (*S*)-2-amino-*N*-methyl-*N*,3-diphenylpropanamide (TFA salt, 184 mg, 0.50 mmol, 1.2 equiv.) were used as starting materials. Yield 77%. ^1H NMR (600 MHz, CD_3OD) δ 7.85 (s, 1H), 7.31 – 7.29 (m, 4H), 7.19 – 7.15 (m, 3H), 6.91 – 6.87 (m, 3H), 5.06 – 5.00 (m, 2H), 4.66 (t, J = 7.4 Hz, 1H), 3.53 (s, 3H), 3.30 (s, 3H), 3.17 (s, 3H), 2.98 (dd, J = 13.4, 7.4 Hz, 1H), 2.75 (dd, J = 13.4, 7.5 Hz, 1H); ^{13}C NMR (150 MHz, CD_3OD) δ 172.9, 168.1, 156.5, 153.2, 149.7, 144.6, 143.8, 137.9, 130.8, 130.2, 129.5, 129.3, 128.6, 127.9, 108.4, 53.4, 49.5, 39.3, 38.1, 30.2, 28.2; HRMS (ESI) m/z calcd for $\text{C}_{25}\text{H}_{25}\text{N}_6\text{O}_4$ $[\text{M} - \text{H}]^-$ 473.1943, found 473.1945.

(S)-2-(2-(1,3-Dimethyl-2,6-dioxo-1,2,3,6-tetrahydro-7H-purin-7-yl)acetamido)-N-methyl-3-phenyl-N-(p-tolyl)propanamide (38): The synthetic method was similar to that of compound **1** except that 2-(1,3-dimethyl-2,6-dioxo-1,2,3,6-tetrahydro-7H-purin-7-yl)acetic acid (100 mg, 0.42 mmol, 1 equiv.) and (S)-2-amino-N-methyl-3-phenyl-N-(p-tolyl)propanamide (TFA salt, 191 mg, 0.50 mmol, 1.2 equiv.) were used as starting materials. Yield 72%. ¹H NMR (600 MHz, CD₃OD) δ 7.82 (s, 1H), 7.14 – 7.07 (m, 5H), 6.87 – 6.77 (m, 4H), 5.00 (s, 2H), 4.66 (t, *J* = 7.4 Hz, 1H), 3.47 (s, 3H), 3.24 (s, 3H), 3.13 (s, 3H), 2.94 (dd, *J* = 13.4, 7.3 Hz, 1H), 2.72 (dd, *J* = 13.4, 7.5 Hz, 1H), 2.27 (s, 3H); ¹³C NMR (100 MHz, CD₃OD) δ 172.9, 168.0, 156.4, 153.2, 149.7, 144.6, 141.2, 139.5, 137.9, 131.3, 130.2, 129.4, 128.2, 127.9, 108.4, 53.3, 39.4, 38.1, 30.2, 28.2, 21.1; HRMS (ESI) *m/z* calcd for C₂₆H₂₇N₆O₄ [M – H][–] 487.2100, found 487.2104.

(S)-2-(2-(1,3-Dimethyl-2,6-dioxo-1,2,3,6-tetrahydro-7H-purin-7-yl)acetamido)-N-(4-fluorophenyl)-N-methyl-3-phenylpropanamide (39): The synthetic method was similar to that of compound **1** except that 2-(1,3-dimethyl-2,6-dioxo-1,2,3,6-tetrahydro-7H-purin-7-yl)acetic acid (100 mg, 0.42 mmol, 1 equiv.) and (S)-2-amino-N-(4-fluorophenyl)-N-methyl-3-phenylpropanamide (TFA salt, 193 mg, 0.50 mmol, 1.2 equiv.) were used as starting materials. Yield 67%. ¹H NMR (600 MHz, CD₃OD) δ 8.53 (d, *J* = 7.5 Hz, 1H), 7.85 (s, 1H), 7.21 – 7.20 (m, 3H), 7.01 – 6.93 (m, 5H), 5.06 – 5.00 (m, 2H), 4.61 (q, *J* = 7.4 Hz, 1H), 3.52 (s, 3H), 3.29 (s, 3H), 3.13 (s, 3H), 2.99 (dd, *J* = 13.2, 8.1 Hz, 1H), 2.78 (dd, *J* = 13.3, 7.0 Hz, 1H); ¹³C NMR (150 MHz, CD₃OD) δ 172.9, 168.0, 163.3 (d, *J* = 247.0 Hz), 156.4, 153.2, 149.7, 144.6, 139.9 (d, *J* = 3.2 Hz), 137.8, 130.6, 130.3, 129.6, 128.0, 117.3 (d, *J* = 23.0 Hz), 108.4, 53.3, 49.4, 39.4, 38.1, 30.2, 28.2; HRMS (ESI) *m/z* calcd for C₂₅H₂₄FN₆O₄ [M – H][–] 491.1849, found 491.1845.

(S)-2-(2-(1,3-Dimethyl-2,6-dioxo-1,2,3,6-tetrahydro-7H-purin-7-yl)acetamido)-N-(3-fluorophenyl)-N-methyl-3-phenylpropanamide (40): The synthetic method was similar to that of compound **1** except that 2-(1,3-dimethyl-2,6-dioxo-1,2,3,6-tetrahydro-7H-purin-7-yl)acetic acid (100 mg, 0.42 mmol, 1 equiv.) and (S)-2-amino-N-(3-fluorophenyl)-N-methyl-3-phenylpropanamide (TFA salt, 193 mg, 0.50 mmol, 1.2 equiv.) were used as starting materials. Yield 75%. ¹H NMR (600 MHz, CD₃OD) δ 8.57 (d, *J* = 7.3 Hz, 1H), 7.86 (s, 1H), 7.29 – 7.20 (m, 4H), 7.03 (t, *J* = 8.3 Hz, 1H), 6.94 – 6.93 (m, 2H), 6.71 – 6.54 (m, 1H), 5.04 (s, 2H), 4.67 – 4.63 (m, 1H), 3.52 (s, 3H), 3.30 (s, 3H), 3.14 (s, 3H), 2.99 (dd, *J* = 13.1, 8.4 Hz, 1H), 2.79 (dd, *J* = 13.2, 6.7 Hz, 1H); ¹³C NMR (150 MHz, CD₃OD) δ 172.7, 168.0, 164.1 (d, *J* = 247.4 Hz), 156.5, 153.2, 149.7, 145.2 (d, *J* = 9.6 Hz), 144.6, 137.7, 132.0 (d, *J* = 9.2 Hz), 130.3, 129.6, 128.0, 124.6, 116.1 (d, *J* = 21.2 Hz), 115.9 (d, *J* = 22.6 Hz), 108.4, 53.4, 49.4, 39.6, 37.9, 30.2, 28.2; HRMS (ESI) *m/z* calcd for C₂₅H₂₄FN₆O₄ [M – H][–] 491.1849, found 491.1843.

(S)-N-(4-Chlorophenyl)-2-(2-(1,3-dimethyl-2,6-dioxo-1,2,3,6-tetrahydro-7H-purin-7-yl)acetamido)-N-methyl-3-phenylpropanamide (41): The synthetic method was similar to that of compound **1** except that 2-(1,3-dimethyl-2,6-dioxo-1,2,3,6-tetrahydro-7H-purin-7-yl)acetic acid (100 mg, 0.42 mmol, 1 equiv.) and (S)-2-amino-N-(4-chlorophenyl)-N-methyl-3-phenylpropanamide (TFA salt, 201 mg, 0.50 mmol, 1.2 equiv.) were used as starting materials. Yield 90%. ¹H NMR (600 MHz, CDCl₃) δ 7.67 (d, *J* = 8.1 Hz, 1H), 7.63

(s, 1H), 7.27 – 7.25 (m, 2H), 7.20 – 7.15 (m, 3H), 6.90 – 6.89 (m, 2H), 6.75 (s, 1H), 4.98 – 4.87 (m, 2H), 4.78 (q, $J = 7.7$ Hz, 1H), 3.59 (s, 3H), 3.37 (s, 3H), 3.18 (s, 3H), 2.96 (dd, $J = 13.4, 7.9$ Hz, 1H), 2.80 (dd, $J = 13.4, 7.1$ Hz, 1H); ^{13}C NMR (100 MHz, CDCl_3) δ 171.2, 165.2, 155.5, 151.5, 148.7, 142.3, 140.8, 135.8, 134.1, 129.9, 129.2, 128.7, 128.4, 127.0, 106.8, 51.4, 49.2, 39.0, 37.7, 29.8, 29.7, 28.0; HRMS (ESI) m/z calcd for $\text{C}_{25}\text{H}_{24}\text{ClN}_6\text{O}_4$ $[\text{M} - \text{H}]^-$ 507.1553, found 507.1548.

(S)-N-(3-Chlorophenyl)-2-(2-(1,3-dimethyl-2,6-dioxo-1,2,3,6-tetrahydro-7H-purin-7-yl)acetamido)-N-methyl-3-phenylpropanamide (42).: The synthetic method was similar to that of compound **1** except that 2-(1,3-dimethyl-2,6-dioxo-1,2,3,6-tetrahydro-7H-purin-7-yl)acetic acid (100 mg, 0.42 mmol, 1 equiv.) and (*S*)-2-amino-*N*-(3-chlorophenyl)-*N*-methyl-3-phenylpropanamide (TFA salt, 201 mg, 0.50 mmol, 1.2 equiv.) were used as starting materials. Yield 82%. ^1H NMR (600 MHz, CDCl_3) δ 7.63 (s, 1H), 7.50 (d, $J = 8.0$ Hz, 1H), 7.28 – 7.17 (m, 5H), 6.90 – 6.89 (m, 3H), 6.58 (s, 1H), 4.96 – 4.84 (m, 2H), 4.79 – 4.75 (m, 1H), 3.59 (s, 3H), 3.38 (s, 3H), 3.17 (s, 3H), 2.95 (dd, $J = 13.3, 8.3$ Hz, 1H), 2.80 (dd, $J = 13.3, 6.8$ Hz, 1H); ^{13}C NMR (100 MHz, CDCl_3) δ 170.9, 164.9, 155.5, 151.5, 148.8, 143.4, 142.2, 135.6, 135.0, 130.6, 129.1, 128.5, 127.5, 127.1, 125.7, 106.8, 51.4, 49.4, 39.1, 37.6, 29.8, 28.0; HRMS (ESI) m/z calcd for $\text{C}_{25}\text{H}_{24}\text{ClN}_6\text{O}_4$ $[\text{M} - \text{H}]^-$ 507.1553, found 507.1559.

(S)-2-(2-(1,3-Dimethyl-2,6-dioxo-1,2,3,6-tetrahydro-7H-purin-7-yl)acetamido)-N-ethyl-N,3-diphenylpropanamide (43).: The synthetic method was similar to that of compound **1** except that 2-(1,3-dimethyl-2,6-dioxo-1,2,3,6-tetrahydro-7H-purin-7-yl)acetic acid (100 mg, 0.42 mmol, 1 equiv.) and (*S*)-2-amino-*N*-ethyl-*N*,3-diphenylpropanamide (TFA salt, 191 mg, 0.50 mmol, 1.2 equiv.) were used as starting materials. Yield 75%. ^1H NMR (600 MHz, CDCl_3) δ 7.57 (s, 1H), 7.37 – 7.33 (m, 4H), 7.15 – 7.09 (m, 3H), 6.90 – 6.81 (m, 3H), 4.95 – 4.76 (m, 2H), 4.74 – 4.70 (m, 1H), 3.86 – 3.80 (m, 1H), 3.62 – 3.58 (m, 1H), 3.58 (s, 3H), 3.38 (s, 3H), 2.94 (dd, $J = 13.7, 6.7$ Hz, 1H), 2.73 (dd, $J = 13.7, 7.8$ Hz, 1H), 1.09 (t, $J = 7.2$ Hz, 3H); ^{13}C NMR (100 MHz, CDCl_3) δ 170.3, 164.8, 155.5, 151.6, 148.7, 142.0, 140.6, 136.0, 129.7, 129.1, 128.4, 128.4, 128.2, 126.7, 106.7, 51.4, 49.5, 44.7, 38.7, 29.8, 28.0, 12.8; HRMS (ESI) m/z calcd for $\text{C}_{26}\text{H}_{27}\text{N}_6\text{O}_4$ $[\text{M} - \text{H}]^-$ 487.2100, found 487.2105.

2-(2-(2,4-Dioxo-1,3-diazaspiro[4.5]decan-3-yl)acetamido)-N-methyl-N,3-diphenylpropanamide (44).: The synthetic method was similar to that of compound **1** except that 2-(2,4-dioxo-1,3-diazaspiro[4.5]decan-3-yl)acetic acid (100 mg, 0.44 mmol, 1 equiv.) and (*S*)-2-amino-*N*-methyl-*N*,3-diphenylpropanamide (TFA salt, 195 mg, 0.53 mmol, 1.2 equiv.) were used as starting materials. Yield 65%. ^1H NMR (600 MHz, $\text{DMSO}-d_6$) δ 8.65 (s, 1H), 8.53 (d, $J = 7.8$ Hz, 1H), 7.45 – 7.32 (m, 3H), 7.20 – 7.12 (m, 4H), 6.82 – 6.77 (m, 2H), 4.42 – 4.38 (m, 1H), 3.95 – 3.82 (m, 2H), 3.13 (s, 3H), 2.81 (dd, $J = 13.2, 6.2$ Hz, 1H), 2.61 (dd, $J = 13.5, 9.2$ Hz, 1H), 1.64 – 1.59 (m, 4H), 1.57 – 1.45 (m, 5H), 1.29 – 1.24 (m, 1H); ^{13}C NMR (150 MHz, $\text{DMSO}-d_6$) δ 176.9, 171.0, 166.1, 155.8, 143.1, 137.7, 130.0, 129.2, 129.2, 128.6, 128.3, 127.9, 126.9, 61.5, 52.1, 37.8, 37.6, 33.7, 24.8, 21.2; HRMS (ESI) m/z calcd for $\text{C}_{26}\text{H}_{31}\text{N}_4\text{O}_4$ $[\text{M} + \text{H}]^+$ 463.2340, found 463.2337.

2-(2-(2,4-Dioxo-1,3-diazaspiro[4.5]decan-3-yl)acetamido)-N,3-diphenylpropanamide.

(45): The synthetic method was similar to that of compound **1** except that 2-(2,4-dioxo-1,3-diazaspiro[4.5]decan-3-yl)acetic acid (100 mg, 0.44 mmol, 1 equiv.) and (*S*)-2-amino-*N*,3-diphenylpropanamide (TFA salt, 188 mg, 0.53 mmol, 1.2 equiv.) were used as starting materials. Yield 70%. ¹H NMR (600 MHz, DMSO-*d*₆) δ 10.04 (s, 1H), 8.67 (s, 1H), 8.55 (d, *J* = 7.9 Hz, 1H), 7.54 (d, *J* = 7.8 Hz, 2H), 7.30 – 7.24 (m, 4H), 7.20 – 7.15 (m, 1H), 7.04 (t, *J* = 7.4 Hz, 1H), 4.64 – 4.59 (m, 1H), 4.00 – 3.89 (m, 2H), 3.02 (dd, *J* = 13.7, 5.8 Hz, 1H), 2.88 (dd, *J* = 13.7, 8.5 Hz, 1H), 1.65 – 1.55 (m, 4H), 1.54 – 1.46 (m, 5H), 1.29 – 1.25 (m, 1H); ¹³C NMR (150 MHz, DMSO-*d*₆) δ 177.0, 170.1, 166.4, 155.9, 139.1, 137.7, 129.6, 129.1, 128.6, 126.9, 123.9, 119.9, 61.5, 55.4, 38.3, 33.7, 33.7, 24.8, 21.2; HRMS (ESI) *m/z* calcd for C₂₅H₂₉N₄O₄ [M + H]⁺ 449.2183, found 449.2186.

2-(2-(2,4-Dioxo-1,3-diazaspiro[4.5]decan-3-yl)acetamido)-N-(4-methoxyphenyl)-N-methyl-3-phenylpropanamide (46):

The synthetic method was similar to that of compound **1** except that 2-(2,4-dioxo-1,3-diazaspiro[4.5]decan-3-yl)acetic acid (100 mg, 0.44 mmol, 1 equiv.) and (*S*)-2-amino-*N*-(4-methoxyphenyl)-*N*-methyl-3-phenylpropanamide (TFA salt, 211 mg, 0.53 mmol, 1.2 equiv.) were used as starting materials. Yield 62%. ¹H NMR (600 MHz, DMSO-*d*₆) δ 8.65 (s, 1H), 8.50 (d, *J* = 7.9 Hz, 1H), 7.20 – 7.14 (m, 3H), 7.07 – 6.99 (m, 2H), 6.93 (d, *J* = 8.3 Hz, 2H), 6.84 (d, *J* = 7.0 Hz, 2H), 4.41 – 4.35 (m, 1H), 3.95 – 3.79 (m, 2H), 3.76 (s, 3H), 3.08 (s, 3H), 2.83 (dd, *J* = 13.5, 5.3 Hz, 1H), 2.61 (dd, *J* = 13.4, 8.8 Hz, 1H), 1.64 – 1.58 (m, 4H), 1.54 – 1.42 (m, 5H), 1.30 – 1.23 (m, 1H); ¹³C NMR (150 MHz, DMSO-*d*₆) δ 176.9, 171.2, 166.0, 158.9, 155.8, 137.7, 135.8, 129.5, 129.1, 128.8, 128.4, 127.1, 115.3, 114.9, 61.5, 55.9, 55.7, 52.0, 51.8, 37.9, 33.7, 24.9, 21.2; HRMS (ESI) *m/z* calcd for C₂₇H₃₃N₄O₅ [M + H]⁺ 493.2445, found 493.2449.

2-(2-(2,4-Dioxo-1,3-diazaspiro[4.5]decan-3-yl)acetamido)-N-methyl-3-phenyl-N-(*p*-tolyl)propanamide (47):

The synthetic method was similar to that of compound **1** except that 2-(2,4-dioxo-1,3-diazaspiro[4.5]decan-3-yl)acetic acid (100 mg, 0.44 mmol, 1 equiv.) and (*S*)-2-amino-*N*-methyl-3-phenyl-*N*-(*p*-tolyl)propanamide (TFA salt, 203 mg, 0.53 mmol, 1.2 equiv.) were used as starting materials. Yield 61%. ¹H NMR (600 MHz, DMSO-*d*₆) δ 8.65 (s, 1H), 8.50 (d, *J* = 7.9 Hz, 1H), 7.20 – 7.15 (m, 4H), 6.98 (d, *J* = 7.1 Hz, 2H), 6.85 – 6.80 (m, 2H), 4.44 – 4.39 (m, 1H), 3.96 – 3.82 (m, 2H), 3.09 (s, 3H), 2.82 (dd, *J* = 12.5, 7.4 Hz, 1H), 2.61 (dd, *J* = 13.2, 8.9 Hz, 1H), 2.31 (s, 3H), 1.66 – 1.59 (m, 4H), 1.54 – 1.44 (m, 5H), 1.31 – 1.24 (m, 1H); ¹³C NMR (150 MHz, DMSO-*d*₆) δ 176.9, 171.0, 166.0, 155.8, 140.6, 137.7, 137.7, 130.5, 129.7, 129.3, 128.6, 127.6, 126.9, 61.5, 51.9, 38.0, 37.6, 33.7, 24.8, 21.2, 21.1; HRMS (ESI) *m/z* calcd for C₂₇H₃₃N₄O₄ [M + H]⁺ 477.2496, found 477.2494.

2-(2-(2,4-Dioxo-1,3-diazaspiro[4.5]decan-3-yl)acetamido)-N-(4-fluorophenyl)-N-methyl-3-phenylpropanamide (48):

The synthetic method was similar to that of compound **1** except that 2-(2,4-dioxo-1,3-diazaspiro[4.5]decan-3-yl)acetic acid (100 mg, 0.44 mmol, 1 equiv.) and (*S*)-2-amino-*N*-(4-fluorophenyl)-*N*-methyl-3-phenylpropanamide (TFA salt, 205 mg, 0.53 mmol, 1.2 equiv.) were used as starting materials. Yield 69%. ¹H NMR (600 MHz, CD₃OD) δ 7.32 – 7.23 (m, 5H), 7.03 – 7.00 (m, 2H), 6.98 – 6.96 (m, 2H),

4.60 – 4.58 (m, 1H), 4.16 – 4.04 (m, 2H), 3.13 (s, 3H), 2.97 (dd, $J = 13.1, 8.4$ Hz, 1H), 2.75 (dd, $J = 13.1, 6.6$ Hz, 1H), 1.83 – 1.77 (m, 4H), 1.66 – 1.63 (m, 3H), 1.58 – 1.53 (m, 2H), 1.43 – 1.37 (m, 1H); ^{13}C NMR (150 MHz, CD_3OD) δ 172.9, 168.0, 163.3 (d, $J = 246.8$ Hz), 157.7, 139.9, 139.9, 137.9, 130.6 (d, $J = 7.6$ Hz), 130.4, 129.6, 128.0, 117.4 (d, $J = 23.0$ Hz), 63.3, 53.2, 40.9, 39.6, 38.1, 34.6, 25.8, 22.5; HRMS (ESI) m/z calcd for $\text{C}_{26}\text{H}_{28}\text{FN}_4\text{O}_4$ [$\text{M} - \text{H}$] $^-$ 479.2100, found 479.2106.

2-(2-(2,4-Dioxo-1,3-diazaspiro[4.5]decan-3-yl)acetamido)-N-(3-fluorophenyl)-N-methyl-3-phenylpropanamide (49).

The synthetic method was similar to that of compound **1** except that 2-(2,4-dioxo-1,3-diazaspiro[4.5]decan-3-yl)acetic acid (100 mg, 0.44 mmol, 1 equiv.) and (*S*)-2-amino-*N*-(3-fluorophenyl)-*N*-methyl-3-phenylpropanamide (TFA salt, 205 mg, 0.53 mmol, 1.2 equiv.) were used as starting materials. Yield 70%. ^1H NMR (600 MHz, CD_3OD) δ 7.33 – 7.23 (m, 5H), 7.06 (t, $J = 8.3$ Hz, 1H), 6.97 – 6.96 (m, 2H), 6.73 (s, 1H), 6.47 (s, 1H), 4.64 – 4.61 (m, 1H), 4.17 – 4.05 (m, 2H), 3.14 (s, 3H), 2.97 (dd, $J = 13.0, 8.6$ Hz, 1H), 2.77 (dd, $J = 13.1, 6.4$ Hz, 1H), 1.84 – 1.79 (m, 4H), 1.67 – 1.64 (m, 3H), 1.59 – 1.52 (m, 2H), 1.43 – 1.37 (m, 1H); ^{13}C NMR (150 MHz, CD_3OD) δ 178.9, 172.7, 168.1, 164.2 (d, $J = 247.4$ Hz), 157.8, 145.3 (d, $J = 9.6$ Hz), 137.8, 132.1 (d, $J = 9.1$ Hz), 130.4, 129.6, 128.1, 124.6, 116.1 (d, $J = 21.1$ Hz), 115.8 (d, $J = 22.9$ Hz), 63.3, 53.4, 40.9, 39.8, 37.9, 34.6, 25.8, 22.5; HRMS (ESI) m/z calcd for $\text{C}_{26}\text{H}_{28}\text{FN}_4\text{O}_4$ [$\text{M} - \text{H}$] $^-$ 479.2100, found 479.2100.

N-(4-Chlorophenyl)-2-(2-(2,4-dioxo-1,3-diazaspiro[4.5]decan-3-yl)acetamido)-N-methyl-3-phenylpropanamide (50).

The synthetic method was similar to that of compound **1** except that 2-(2,4-dioxo-1,3-diazaspiro[4.5]decan-3-yl)acetic acid (100 mg, 0.44 mmol, 1 equiv.) and (*S*)-2-amino-*N*-(4-chlorophenyl)-*N*-methyl-3-phenylpropanamide (TFA salt, 213 mg, 0.53 mmol, 1.2 equiv.) were used as starting materials. Yield 56%. ^1H NMR (400 MHz, $\text{DMSO}-d_6$) δ 8.67 (s, 1H), 8.60 (d, $J = 7.7$ Hz, 1H), 7.45 (d, $J = 8.5$ Hz, 2H), 7.22 – 7.18 (m, 3H), 7.10 (d, $J = 8.1$ Hz, 2H), 6.91 – 6.87 (m, 2H), 4.40 – 4.32 (m, 1H), 3.98 – 3.82 (m, 2H), 2.90 – 2.83 (m, 1H), 2.66 (dd, $J = 13.2, 8.3$ Hz, 1H), 1.70 – 1.60 (m, 4H), 1.56 – 1.41 (m, 5H), 1.31 – 1.28 (m, 1H); ^{13}C NMR (100 MHz, $\text{DMSO}-d_6$) δ 177.0, 170.9, 166.2, 155.8, 142.0, 137.5, 132.8, 130.0, 129.8, 129.3, 128.7, 127.1, 61.6, 52.0, 38.0, 37.5, 33.7, 24.8, 21.3; HRMS (ESI) m/z calcd for $\text{C}_{26}\text{H}_{30}\text{ClN}_4\text{O}_4$ [$\text{M} + \text{H}$] $^+$ 497.1950, found 497.1952.

N-(3-Chlorophenyl)-2-(2-(2,4-dioxo-1,3-diazaspiro[4.5]decan-3-yl)acetamido)-N-methyl-3-phenylpropanamide (51).

The synthetic method was similar to that of compound **1** except that 2-(2,4-dioxo-1,3-diazaspiro[4.5]decan-3-yl)acetic acid (100 mg, 0.44 mmol, 1 equiv.) and (*S*)-2-amino-*N*-(3-chlorophenyl)-*N*-methyl-3-phenylpropanamide (TFA salt, 213 mg, 0.53 mmol, 1.2 equiv.) were used as starting materials. Yield 72%. ^1H NMR (600 MHz, CD_3OD) δ 7.32 – 7.25 (m, 7H), 6.98 – 6.96 (m, 2H), 4.60 – 4.58 (m, 1H), 4.17 – 4.05 (m, 2H), 3.12 (s, 3H), 2.97 (dd, $J = 13.0, 9.0$ Hz, 1H), 2.77 (dd, $J = 13.0, 6.2$ Hz, 1H), 1.84 – 1.78 (m, 4H), 1.68 – 1.64 (m, 3H), 1.59 – 1.53 (m, 2H), 1.44 – 1.37 (m, 1H); HRMS-ESI ($-$) m/z calcd for $\text{C}_{26}\text{H}_{28}\text{ClN}_4\text{O}_4$ [$\text{M} - \text{H}$] $^-$ 495.1805, found 495.1810.

N-(3-Bromophenyl)-2-(2-(2,4-dioxo-1,3-diazaspiro[4.5]decan-3-yl)acetamido)-N-methyl-3-phenylpropanamide (52). The synthetic method was similar to that of compound **1** except that 2-(2,4-dioxo-1,3-diazaspiro[4.5]decan-3-yl)acetic acid (100 mg, 0.44 mmol, 1 equiv.) and (*S*)-2-amino-*N*-(3-bromophenyl)-*N*-methyl-3-phenylpropanamide (TFA salt, 237 mg, 0.53 mmol, 1.2 equiv.) were used as starting materials. Yield 68%. ¹H NMR (600 MHz, DMSO-*d*₆) δ 8.65 (s, 1H), 8.60 (d, *J* = 7.3 Hz, 1H), 7.54 (d, *J* = 7.9 Hz, 1H), 7.33 (t, *J* = 8.0 Hz, 1H), 7.20 – 7.13 (m, 5H), 6.88 – 6.87 (m, 2H), 4.34 – 4.31 (m, 1H), 3.95 – 3.84 (m, 2H), 3.08 (s, 3H), 2.86 (dd, *J* = 13.4, 5.9 Hz, 1H), 2.66 (dd, *J* = 14.4, 7.2 Hz, 1H), 1.63 – 1.48 (m, 9H), 1.29 – 1.23 (m, 1H); ¹³C NMR (100 MHz, DMSO-*d*₆) δ 177.0, 171.0, 166.2, 155.8, 144.6, 137.5, 131.7, 131.3, 130.7, 129.3, 128.8, 127.2, 127.1, 122.3, 61.6, 52.2, 38.1, 37.5, 33.7, 24.9, 21.3; HRMS (ESI) *m/z* calcd for C₂₆H₂₈BrN₄O₄ [M – H][–] 539.1299, found 539.1297.

2-(2-(2,4-Dioxo-1,3-diazaspiro[4.5]decan-3-yl)acetamido)-N-ethyl-N,3-diphenylpropanamide (53). The synthetic method was similar to that of compound **1** except that 2-(2,4-dioxo-1,3-diazaspiro[4.5]decan-3-yl)acetic acid (100 mg, 0.44 mmol, 1 equiv.) and (*S*)-2-amino-*N*-ethyl-*N*,3-diphenylpropanamide (TFA salt, 203 mg, 0.53 mmol, 1.2 equiv.) were used as starting materials. Yield 58%. ¹H NMR (400 MHz, DMSO-*d*₆) δ 8.65 (s, 1H), 8.49 (d, *J* = 7.9 Hz, 1H), 7.46 – 7.39 (m, 3H), 7.20 – 7.16 (m, 3H), 7.08 – 7.04 (m, 2H), 6.86 – 6.81 (m, 2H), 4.35 – 4.28 (m, 1H), 3.98 – 3.83 (m, 2H), 3.69 – 3.55 (m, 2H), 2.86 (dd, *J* = 13.4, 5.5 Hz, 1H), 2.62 (dd, *J* = 13.4, 8.5 Hz, 1H), 1.65 – 1.53 (m, 4H), 1.56 – 1.45 (m, 5H), 1.34 – 1.25 (m, 1H), 0.97 (t, *J* = 7.1 Hz, 3H); ¹³C NMR (100 MHz, DMSO-*d*₆) δ 170.0, 170.4, 166.0, 155.8, 141.3, 137.7, 130.0, 129.4, 128.9, 128.6, 128.5, 127.0, 61.5, 52.3, 44.2, 38.0, 33.7, 24.9, 21.3, 13.1; HRMS (ESI) *m/z* calcd for C₂₇H₃₃N₄O₄ [M + H]⁺ 477.2496, found 477.2500.

2-(2-(2,5-Dioxo-3',4'-dihydro-2'H-spiro[imidazolidine-4,1'-naphthalen]-1-yl)acetamido)-N-methyl-N,3-diphenylpropanamide (54). The synthetic method was similar to that of compound **1** except that 2-(2,5-dioxo-3',4'-dihydro-2'*H*-spiro[imidazolidine-4,1'-naphthalen]-1-yl)acetic acid (100 mg, 0.36 mmol, 1 equiv.) and (*S*)-2-amino-*N*-methyl-*N*,3-diphenylpropanamide (TFA salt, 158 mg, 0.43 mmol, 1.2 equiv.) were used as starting materials. Yield 52%. ¹H NMR (600 MHz, DMSO-*d*₆) δ 8.83 (s, 1H), 8.63 (d, *J* = 8.0 Hz, 1H), 7.46 – 7.32 (m, 3H), 7.31 – 7.04 (m, 9H), 6.84 (d, *J* = 6.4 Hz, 2H), 4.46 – 4.41 (m, 1H), 4.09 – 3.94 (m, 2H), 3.12 (s, 3H), 2.86 (dd, *J* = 13.3, 5.3 Hz, 1H), 2.75 – 2.60 (m, 2H), 2.63 – 2.60 (m, 1H), 2.09 – 1.82 (m, 4H); HRMS (ESI) *m/z* calcd for C₃₀H₃₁N₄O₄ [M + H]⁺ 511.2340, found 511.2340.

2-(2-(2,5-Dioxo-3',4'-dihydro-2'H-spiro[imidazolidine-4,1'-naphthalen]-1-yl)acetamido)-N,3-diphenylpropanamide (55). The synthetic method was similar to that of compound **1** except that 2-(2,5-dioxo-3',4'-dihydro-2'*H*-spiro[imidazolidine-4,1'-naphthalen]-1-yl)acetic acid (100 mg, 0.36 mmol, 1 equiv.) and (*S*)-2-amino-*N*,3-diphenylpropanamide (TFA salt, 152 mg, 0.43 mmol, 1.2 equiv.) were used as starting materials. Yield 72%. ¹H NMR (600 MHz, DMSO-*d*₆) δ 10.09 (s, 1H), 8.87 (s, 1H), 8.68 (s, 1H), 7.54 (s, 2H), 7.26 – 6.94 (m, 10H), 4.72 (s, 1H), 4.15 – 4.05 (m, 2H), 3.05 (s, 2H), 2.91 (s, 1H), 2.76 (s, 2H), 2.08 – 1.81 (m, 4H); ¹³C NMR (150 MHz, DMSO-*d*₆) δ 176.6, 170.0,

166.4, 155.7, 139.0, 138.1, 137.7, 134.6, 129.6, 129.6, 129.5, 129.1, 128.6, 128.5, 128.0, 119.9, 126.9, 123.9, 62.8, 55.4, 38.5, 34.1, 28.9, 18.9; HRMS (ESI) m/z calcd for $C_{29}H_{29}N_4O_4$ $[M + H]^+$ 497.2183, found 497.2182.

2-(2-(2,5-Dioxo-3',4'-dihydro-2'H-spiro[imidazolidine-4,1'-naphthalen]-1-yl)acetamido)-N-(4-methoxyphenyl)-N-methyl-3-phenylpropanamide (56): The synthetic method was similar to that of compound **1** except that 2-(2,5-dioxo-3',4'-dihydro-2'H-spiro[imidazolidine-4,1'-naphthalen]-1-yl)acetic acid (100 mg, 0.36 mmol, 1 equiv.) and (*S*)-2-amino-*N*-(4-methoxyphenyl)-*N*-methyl-3-phenylpropanamide (TFA salt, 171 mg, 0.43 mmol, 1.2 equiv.) were used as starting materials. Yield 67%. 1H NMR (600 MHz, DMSO- d_6) δ 8.83 (s, 1H), 8.61 – 8.57 (m, 1H), 7.25 – 7.11 (m, 7H), 7.06 – 6.96 (m, 2H), 6.95 – 6.92 (m, 2H), 6.91 – 6.86 (m, 2H), 4.44 – 4.34 (m, 1H), 4.10 – 3.98 (m, 2H), 3.77 (s, 3H), 3.08 (s, 3H), 2.87 (dd, J = 13.1, 5.5 Hz, 1H), 2.77 – 2.75 (m, 2H), 2.66 – 2.61 (m, 1H), 2.15 – 2.02 (m, 2H), 1.92 – 1.80 (m, 2H); HRMS (ESI) m/z calcd for $C_{31}H_{33}N_4O_5$ $[M + H]^+$ 541.2445, found 541.2446.

2-(2-(2,5-Dioxo-3',4'-dihydro-2'H-spiro[imidazolidine-4,1'-naphthalen]-1-yl)acetamido)-N-methyl-3-phenyl-N-(p-tolyl)propanamide (57): The synthetic method was similar to that of compound **1** except that 2-(2,5-dioxo-3',4'-dihydro-2'H-spiro[imidazolidine-4,1'-naphthalen]-1-yl)acetic acid (100 mg, 0.36 mmol, 1 equiv.) and (*S*)-2-amino-*N*-methyl-3-phenyl-*N*-(*p*-tolyl)propanamide (TFA salt, 164 mg, 0.43 mmol, 1.2 equiv.) were used as starting materials. Yield 55%. 1H NMR (600 MHz, DMSO- d_6) δ 8.83 (s, 1H), 8.60 (d, J = 7.9 Hz, 1H), 7.29 (d, J = 7.8 Hz, 1H), 7.29 – 7.12 (m, 8H), 6.95 (d, J = 7.1 Hz, 2H), 6.87 (d, J = 7.4 Hz, 2H), 4.46 – 4.40 (m, 1H), 4.13 – 3.92 (m, 2H), 3.08 (s, 3H), 2.87 (dd, J = 13.5, 5.8 Hz, 1H), 2.77 – 2.72 (m, 2H), 2.64 (dd, J = 13.3, 8.4 Hz, 1H), 2.32 (s, 3H), 2.08 – 1.80 (m, 4H); ^{13}C NMR (150 MHz, DMSO- d_6) δ 176.6, 171.0, 166.0, 155.7, 138.1, 137.7, 137.6, 134.6, 130.4, 129.5, 129.4, 128.6, 128.5, 127.6, 126.9, 62.7, 51.8, 38.1, 37.6, 34.0, 28.9, 21.1, 18.9; HRMS (ESI) m/z calcd for $C_{31}H_{33}N_4O_4$ $[M + H]^+$ 525.2496, found 525.2498.

4.2 Thermal Shift Assays (TSAs) to test compounds for HIV-1 CA hexamer stability

Compounds were screened for their effect on CA stability using purified covalently-crosslinked hexameric CA^{A14C/E45C/W184A/M185A} (CA121). CA121 cloned in a pET11a expression plasmid was kindly provided by Dr. Owen Pornillos (University of Virginia, Charlottesville, VA). Protein was expressed in *E. coli* BL21(DE3)RIL and purified as reported previously [34]. The TSA has been previously described [56–58]. Briefly, the TSA was conducted on the PikoReal Real-Time PCR System (Thermo Fisher Scientific) or the QuantStudio 3 Real-Time PCR system (Thermo Fisher Scientific). Each reaction contained 7.5 μ M CA121, 1x Sypro Orange Protein Gel Stain (Life Technologies), 50 mM sodium phosphate buffer (pH 8.0) and 1% DMSO (control) or 20 μ M compound. The plate was heated from 25 to 95 °C with a heating rate of 0.2 °C every 10 sec. The fluorescence intensity was measured with an Ex range of 475–500 nm and Em range of 520–590 nm. The differences in the melting temperature (T_m) of CA hexamer in DMSO (T_0) verses in the presence of compound (T_m) were calculated using the following formula: $T_m = T_m - T_0$.

4.3 Virus Production

The wild-type laboratory HIV-1 strain, HIV-1_{NL4-3} [59], was produced using a pNL4-3 vector that was obtained through the NIH AIDS Reagent Program, Division of AIDS, NIAID, NIH. HIV-1_{NL4-3} was generated by transfecting HEK 293FT cells in a T75 flask with 10 µg of the pNL4-3 vector and FuGENE®HD Transfection Reagent (Promega). Supernatant was harvested 48–72 hours post-transfection and transferred to MT2 cells for viral propagation. Virus was harvested when syncytia formation was observed, which took 3–5 days. The viral supernatant was then concentrated using 8% w/v PEG 8,000 overnight at 4 °C, followed by centrifugation for 40 min at 3,500 rpm. The resulting viral-containing pellet was concentrated 10-fold by resuspension in DMEM without FBS and stored at –80 °C.

4.4 Anti-HIV-1 and Cytotoxicity assays

Anti-HIV-1 activity of PF74 and PF74-related analogs were examined in TZM-GFP cells. The potency of HIV-1 inhibition by a compound was based on its inhibitory effect on viral LTR-activated GFP expression compared with that of compound-free (DMSO) controls. Briefly, TZM-GFP cells were plated at density of 1×10^4 cells per well in a 96-well plate. 24 h later, media was replaced with increasing concentrations of compound. 24 h post treatment, cells were exposed to an HIV-1 strain (MOI = 1). After incubation for 48 h, anti-HIV-1 activity was assessed by counting the number of GFP positive cells on a Cytation™ 5 Imaging Reader (BioTek) and 50% effective concentration (EC₅₀) values were determined.

Cytotoxicity of each compound was also determined in TZM-GFP cells. Cells were plated at a density of 1×10^4 cells per well in a 96-well plate and were continuously exposed to increasing concentrations of a compound for 72 hours. The number of viable cells in each well was determined using a Cell Proliferation Kit II (XTT), and 50% cytotoxicity concentration (CC₅₀) values were determined. All the cell-based assays were conducted in duplicate and in at least two independent experiments.

For the EC₅₀ and CC₅₀ dose responses, values were plotted in GraphPad Prism 5 and analyzed with the *log (inhibitor) vs. normalized response – variable slope* equation. Final values were calculated in each independent assay and the average values were determined. Statistical analysis (calculation of standard deviation) was performed by using Microsoft Excel.

4.5 Microsomal stability assay.

The *in vitro* microsomal stability assay was conducted in duplicate in mouse and human liver microsomal systems, which were supplemented with nicotinamide adenine dinucleotide phosphate (NADPH) as a cofactor. Briefly, a compound (1 µM final concentration) was pre-incubated, in the absence or presence of 0.5 µM Cobicistat (CYP 3A inhibitor, purchased from medchemexpress.com and verified with LCMS), with the reaction mixture containing liver microsomal protein (0.5 mg/mL final concentration) and MgCl₂ (1 mM final concentration) in 0.1 M potassium phosphate buffer (pH 7.4) at 37 °C for 15 minutes. The reaction was initiated by addition of 1 mM NADPH, followed by incubation at 37 °C. A negative control was performed in parallel in the absence of NADPH to measure any

chemical instability or non-NADPH dependent enzymatic degradation for each compound. At various time points (0, 5, 15, 30, and 60 min), 1 volume of reaction aliquot was taken and quenched with 3 volumes of acetonitrile containing an appropriate internal standard and 0.1% formic acid. The samples were then vortexed and centrifuged at 15,000 rpm for 5 min at 4 °C. The supernatants were collected and analyzed by LC-MS/MS to determine the *in vitro* metabolic half-life ($t_{1/2}$).

4.6 Molecular modeling

Molecular modeling was performed using the Schrödinger small molecule drug discovery suite 2019–1 [60]. The crystal structure of native full length HIV-1 capsid protein in complex with **PF74** was retrieved from the protein data bank (PDB code: 4XFZ) [30]. The above structure was analyzed using Maestro [61] (Schrödinger Inc.) and subjected to a docking protocol that involves several steps including preparing the protein of interest, grid generation, ligand preparation, and docking. The crystal structure was refined using the protein preparation wizard [62] (Schrödinger Inc.) in which missing hydrogen atoms, side chains, and loops were added using prime and minimized using the OPLS 3e force field [63] to optimize the hydrogen bonding network and converge the heavy atoms to an rmsd of 0.3 Å. The receptor grid generation tool in Maestro (Schrödinger Inc.) was used to define an active site around the native ligand **PF74** to cover all the residues within 12 Å. All the compounds were drawn using Maestro and subjected to LigPrep [64] to generate conformers, possible protonation at pH of 7±2 that serves as an input for docking process. All the dockings were performed using Glide XP [65](Glide, version 8.2) with the van der Waals radii of nonpolar atoms for each of the ligands scaled by a factor of 0.8. The solutions were further refined by post docking and minimization under implicit solvent to account for protein flexibility. The residue numbers of HIV-1 capsid protein used in the discussion and the figures were based on the native full length HIV-1 capsid protein.

Supplementary Material

Refer to Web version on PubMed Central for supplementary material.

Acknowledgments

This research was supported by the National Institute of Allergy and Infectious Diseases, the National Institutes of Health, grant number R01AI120860 (to SGS and ZW). We thank the Minnesota Supercomputing Institute for molecular modeling resources.

Abbreviations

HIV	human immunodeficiency virus
CA	capsid protein
CPSF6	cleavage and polyadenylation specific factor 6
CypA	Cyclophilin A
CA_{NTD}	CA N-terminal domain

CA_{CTD}	CA C-terminal domain
SAR	structure-activity-relationship
HATU	1-[Bis(dimethylamino)methylene]-1 <i>H</i> -1,2,3-triazolo[4,5- <i>b</i>]pyridinium 3-oxid hexafluorophosphate
T₃P	2,4,6-Tripropyl-1,3,5,2,4,6-trioxatriphosphorinane-2,4,6-trioxide
DIPEA	<i>N,N</i> -Diisopropylethylamine
TFA	Trifluoroacetic acid
TSA	thermal shift assay
HLM	human liver microsome
MLM	mouse liver microsome
EC₅₀	50% effective concentration
CC₅₀	50% cytotoxicity concentration

References

1. AIDSinfo, 'FDA-Approved HIV Medicines' <<https://aidsinfo.nih.gov/understanding-hiv-aids/fact-sheets/21/58/fda-approved-hiv-medicines>> [Accessed March 2020].
2. Campbell EM, and Hope TJ, HIV-1 capsid: the multifaceted key player in HIV-1 infection, *Nat Rev Microbiol*, 13 (2015), 471–83. [PubMed: 26179359]
3. Le Sage V, Mouland AJ, and Valiente-Echeverria F, Roles of HIV-1 capsid in viral replication and immune evasion, *Virus Res*, 193 (2014), 116–29. [PubMed: 25036886]
4. Fassati A, Multiple roles of the capsid protein in the early steps of HIV-1 infection, *Virus Res*, 170 (2012), 15–24. [PubMed: 23041358]
5. Bell NM, and Lever AM, HIV Gag polyprotein: processing and early viral particle assembly, *Trends Microbiol*, 21 (2013), 136–44. [PubMed: 23266279]
6. Carnes SK, Sheehan JH, and Aiken C, Inhibitors of the HIV-1 capsid, a target of opportunity, *Curr Opin HIV AIDS*, 13 (2018), 359–65. [PubMed: 29782334]
7. Thenin-Houssier S, and Valente ST, HIV-1 Capsid Inhibitors as Antiretroviral Agents, *Curr HIV Res*, 14 (2016), 270–82. [PubMed: 26957201]
8. Zhang JY, Liu XY, and De Clercq E, Capsid (CA) Protein as a Novel Drug Target: Recent Progress in the Research of HIV-1 CA Inhibitors, *Mini-Rev Med Chem*, 9 (2009), 510–18. [PubMed: 19356128]
9. Ganser BK, Li S, Klishko VY, Finch JT, and Sundquist WI, Assembly and analysis of conical models for the HIV-1 core, *Science*, 283 (1999), 80–3. [PubMed: 9872746]
10. Li S, Hill CP, Sundquist WI, and Finch JT, Image reconstructions of helical assemblies of the HIV-1 CA protein, *Nature*, 407 (2000), 409–13. [PubMed: 11014200]
11. Rankovic S, Ramalho R, Aiken C, and Rousso I, **PF74** Reinforces the HIV-1 Capsid To Impair Reverse Transcription-Induced Uncoating, *J Virol*, 92 (2018).
12. Ambrose Z, and Aiken C, HIV-1 uncoating: connection to nuclear entry and regulation by host proteins, *Virology*, 454–455 (2014), 371–9.
13. Yamashita M, and Engelman AN, Capsid-Dependent Host Factors in HIV-1 Infection, *Trends Microbiol*, 25 (2017), 741–55. [PubMed: 28528781]
14. Sayah DM, Sokolskaja E, Berthoux L, and Luban J, Cyclophilin A retrotransposition into TRIM5 explains owl monkey resistance to HIV-1, *Nature*, 430 (2004), 569–73. [PubMed: 15243629]

15. Strelau M, Owens CM, Perron MJ, Kiessling M, Autissier P, and Sodroski J, The cytoplasmic body component TRIM5 α restricts HIV-1 infection in Old World monkeys, *Nature*, 427 (2004), 848–53. [PubMed: 14985764]
16. Achuthan V, Perreira JM, Sowd GA, Puray-Chavez M, McDougall WM, Paulucci-Holthausen A, Wu X, Fadel HJ, Poeschla EM, Multani AS, Hughes SH, Sarafianos SG, Brass AL, and Engelman AN, Capsid-CPSF6 Interaction Licenses Nuclear HIV-1 Trafficking to Sites of Viral DNA Integration, *Cell Host Microbe*, 24 (2018), 392–404 e8. [PubMed: 30173955]
17. Bejarano DA, Peng K, Laketa V, Borner K, Jost KL, Lucic B, Glass B, Lusic M, Mueller B, and Krausslich HG, HIV-1 nuclear import in macrophages is regulated by CPSF6-capsid interactions at the nuclear pore complex, *Elife*, 8 (2019).
18. Woodward CL, Prakobwanakit S, Mosessian S, and Chow SA, Integrase interacts with nucleoporin NUP153 to mediate the nuclear import of human immunodeficiency virus type 1, *J Virol*, 83 (2009), 6522–33. [PubMed: 19369352]
19. Matreyek KA, Yucel SS, Li X, and Engelman A, Nucleoporin NUP153 phenylalanine-glycine motifs engage a common binding pocket within the HIV-1 capsid protein to mediate lentiviral infectivity, *PLoS Pathog*, 9 (2013), e1003693. [PubMed: 24130490]
20. Buffone C, Martinez-Lopez A, Fricke T, Opp S, Severgnini M, Cifola I, Petiti L, Frabetti S, Skorupka K, Zadrozny KK, Ganser-Pornillos BK, Pornillos O, Di Nunzio F, and Diaz-Griffero F, Nup153 Unlocks the Nuclear Pore Complex for HIV-1 Nuclear Translocation in Nondividing Cells, *J Virol*, 92 (2018).
21. Dharan A, Talley S, Tripathi A, Mamede JI, Majetschak M, Hope TJ, and Campbell EM, KIF5B and Nup358 Cooperatively Mediate the Nuclear Import of HIV-1 during Infection, *PLoS Pathog*, 12 (2016), e1005700. [PubMed: 27327622]
22. Meehan AM, Saenz DT, Guevera R, Morrison JH, Peretz M, Fadel HJ, Hamada M, van Deursen J, and Poeschla EM, A cyclophilin homology domain-independent role for Nup358 in HIV-1 infection, *PLoS Pathog*, 10 (2014), e1003969. [PubMed: 24586169]
23. Fricke T, White TE, Schulte B, de Souza Aranha Vieira DA, Dharan A, Campbell EM, Brandariz-Nunez A, and Diaz-Griffero F, MxB binds to the HIV-1 core and prevents the uncoating process of HIV-1, *Retrovirology*, 11 (2014), 68. [PubMed: 25123063]
24. Xu B, Pan Q, and Liang C, Role of MxB in Alpha Interferon-Mediated Inhibition of HIV-1 Infection, *J Virol*, 92 (2018).
25. Franke EK, Yuan HE, and Luban J, Specific incorporation of cyclophilin A into HIV-1 virions, *Nature*, 372 (1994), 359–62. [PubMed: 7969494]
26. Thali M, Bukovsky A, Kondo E, Rosenwirth B, Walsh CT, Sodroski J, and Gottlinger HG, Functional association of cyclophilin A with HIV-1 virions, *Nature*, 372 (1994), 363–5. [PubMed: 7969495]
27. Kim K, Dauphin A, Komurlu S, McCauley SM, Yurkovetskiy L, Carbone C, Diehl WE, Strambio-De-Castillia C, Campbell EM, and Luban J, Cyclophilin A protects HIV-1 from restriction by human TRIM5 α , *Nat Microbiol*, 4 (2019), 2044–51. [PubMed: 31636416]
28. Novikova M, Zhang Y, Freed EO, and Peng K, Multiple Roles of HIV-1 Capsid during the Virus Replication Cycle, *Virology*, 34 (2019), 119–34. [PubMed: 31028522]
29. Freed EO, HIV-1 assembly, release and maturation, *Nat Rev Microbiol*, 13 (2015), 484–96. [PubMed: 26119571]
30. Gres AT, Kirby KA, KewalRamani VN, Tanner JJ, Pornillos O, and Sarafianos SG, STRUCTURAL VIROLOGY. X-ray crystal structures of native HIV-1 capsid protein reveal conformational variability, *Science*, 349 (2015), 99–103. [PubMed: 26044298]
31. Lemke CT, Titolo S, von Schwedler U, Goudreau N, Mercier JF, Wardrop E, Faucher AM, Coulombe R, Banik SS, Fader L, Gagnon A, Kawai SH, Rancourt J, Tremblay M, Yoakim C, Simoneau B, Archambault J, Sundquist WI, and Mason SW, Distinct effects of two HIV-1 capsid assembly inhibitor families that bind the same site within the N-terminal domain of the viral CA protein, *J Virol*, 86 (2012), 6643–55. [PubMed: 22496222]
32. Ternois F, Sticht J, Duquerroy S, Krausslich HG, and Rey FA, The HIV-1 capsid protein C-terminal domain in complex with a virus assembly inhibitor, *Nat Struct Mol Biol*, 12 (2005), 678–82. [PubMed: 16041386]

33. Blair WS, Pickford C, Irving SL, Brown DG, Anderson M, Bazin R, Cao JA, Ciaramella G, Isaacson J, Jackson L, Hunt R, Kjerrstrom A, Nieman JA, Patick AK, Perros M, Scott AD, Whitby K, Wu H, and Butler SL, HIV Capsid is a Tractable Target for Small Molecule Therapeutic Intervention, *Plos Pathogens*, 6 (2010).
34. Pornillos O, Ganser-Pornillos BK, Kelly BN, Hua Y, Whitby FG, Stout CD, Sundquist WI, Hill CP, and Yeager M, X-ray structures of the hexameric building block of the HIV capsid, *Cell*, 137 (2009), 1282–92. [PubMed: 19523676]
35. Zhao G, Perilla JR, Yufenyuy EL, Meng X, Chen B, Ning J, Ahn J, Gronenborn AM, Schulten K, Aiken C, and Zhang P, Mature HIV-1 capsid structure by cryo-electron microscopy and all-atom molecular dynamics, *Nature*, 497 (2013), 643–6. [PubMed: 23719463]
36. Machara A, Lux V, Kozisek M, Grantz Saskova K, Stepanek O, Kotora M, Parkan K, Pavova M, Glass B, Sehr P, Lewis J, Muller B, Krausslich HG, and Konvalinka J, Specific Inhibitors of HIV Capsid Assembly Binding to the C-Terminal Domain of the Capsid Protein: Evaluation of 2-Arylquinazolines as Potential Antiviral Compounds, *J Med Chem*, 59 (2016), 545–58. [PubMed: 26685880]
37. Thenin-Houssier S, de Vera IM, Pedro-Rosa L, Brady A, Richard A, Konnick B, Opp S, Buffone C, Fuhrmann J, Kota S, Billack B, Pietka-Ottlik M, Tellinghuisen T, Choe H, Spicer T, Scampavia L, Diaz-Griffero F, Kojetin DJ, and Valente ST, Ebselen, a Small-Molecule Capsid Inhibitor of HIV-1 Replication, *Antimicrob Agents Chemother*, 60 (2016), 2195–208. [PubMed: 26810656]
38. Kelly BN, Kyere S, Kinde I, Tang C, Howard BR, Robinson H, Sundquist WI, Summers MF, and Hill CP, Structure of the antiviral assembly inhibitor CAP-1 complex with the HIV-1 CA protein, *J Mol Biol*, 373 (2007), 355–66. [PubMed: 17826792]
39. Goudreau N, Lemke CT, Faucher AM, Grand-Maitre C, Goulet S, Lacoste JE, Rancourt J, Malenfant E, Mercier JF, Titolo S, and Mason SW, Novel inhibitor binding site discovery on HIV-1 capsid N-terminal domain by NMR and X-ray crystallography, *ACS Chem Biol*, 8 (2013), 1074–82. [PubMed: 23496828]
40. Liu Z, Pan Q, Liang Z, Qiao W, Cen S, and Liang C, The highly polymorphic cyclophilin A-binding loop in HIV-1 capsid modulates viral resistance to MxB, *Retrovirology*, 12 (2015), 1. [PubMed: 25571928]
41. Lamorte L, Titolo S, Lemke CT, Goudreau N, Mercier JF, Wardrop E, Shah VB, von Schwedler UK, Langelier C, Banik SSR, Aiken C, Sundquist WI, and Mason SW, Discovery of Novel Small-Molecule HIV-1 Replication Inhibitors That Stabilize Capsid Complexes, *Antimicrob Agents Ch*, 57 (2013), 4622–31.
42. Yant SR, Mulato A, Hansen D, Tse WC, Niedziela-Majka A, Zhang JR, Stepan GJ, Jin D, Wong MH, Perreira JM, Singer E, Papalia GA, Hu EY, Zheng J, Lu B, Schroeder SD, Chou K, Ahmadyar S, Liclican A, Yu H, Novikov N, Paoli E, Gonik D, Ram RR, Hung M, McDougall WM, Brass AL, Sundquist WI, Cihlar T, and Link JO, A highly potent long-acting small-molecule HIV-1 capsid inhibitor with efficacy in a humanized mouse model, *Nat Med*, 25 (2019), 1377–84. [PubMed: 31501601]
43. Saito A, Ferhadian D, Sowd GA, Serrao E, Shi J, Halambage UD, Teng S, Soto J, Siddiqui MA, Engelman AN, Aiken C, and Yamashita M, Roles of Capsid-Interacting Host Factors in Multimodal Inhibition of HIV-1 by PF74, *J. Virol*, 90 (2016), 5808–23. [PubMed: 27076642]
44. Shi J, Zhou J, Shah VB, Aiken C, and Whitby K, Small-molecule inhibition of human immunodeficiency virus type 1 infection by virus capsid destabilization, *J Virol*, 85 (2011), 542–9. [PubMed: 20962083]
45. Sun L, Huang T, Dick A, Meuser ME, Zalloum WA, Chen CH, Ding X, Gao P, Cocklin S, Lee KH, Zhan P, and Liu X, Design, synthesis and structure-activity relationships of 4-phenyl-1H-1,2,3-triazole phenylalanine derivatives as novel HIV-1 capsid inhibitors with promising antiviral activities, *Eur J Med Chem*, 190 (2020), 112085. [PubMed: 32066010]
46. Wu G, Zalloum WA, Meuser ME, Jing L, Kang D, Chen CH, Tian Y, Zhang F, Cocklin S, Lee KH, Liu X, and Zhan P, Discovery of phenylalanine derivatives as potent HIV-1 capsid inhibitors from click chemistry-based compound library, *Eur J Med Chem*, 158 (2018), 478–92. [PubMed: 30243152]
47. Sun L, Dick A, Meuser ME, Huang T, Zalloum WA, Chen C-H, Cherukupalli S, Xu S, Ding X, Gao P, Kang D, Clercq ED, Pannecouque C, Cocklin S, Lee K-H, Liu X, and Zhan P, Design,

- Synthesis, and Mechanism Study of Benzenesulfonamide-Containing Phenylalanine Derivatives as Novel HIV-1 Capsid Inhibitors with Improved Antiviral Activities, *J. Med. Chem.*, 63 (2020), 4790–810. [PubMed: 32298111]
48. Wang L, Casey MC, Vernekar SKV, Do HT, Sahani RL, Kirby KA, Du H, Hachiya A, Zhang H, Tedbury PR, Xie J, Sarafianos SG, and Wang Z, Chemical profiling of HIV-1 capsid-targeting antiviral **PF74**, *Eur. J. Med. Chem.*, 200 (2020), 112427. [PubMed: 32438252]
 49. Vernekar SKV, Sahani RL, Casey MC, Kankanala J, Wang L, Kirby KA, Du H, Zhang H, Tedbury PR, Xie J, Sarafianos SG, and Wang Z, Toward Structurally Novel and Metabolically Stable HIV-1 Capsid-Targeting Small Molecules, *Viruses*, 12 (2020).
 50. Xu JP, Francis AC, Meuser ME, Mankowski M, Ptak RG, Rashad AA, Melikyan GB, and Cocklin S, Exploring Modifications of an HIV-1 Capsid Inhibitor: Design, Synthesis, and Mechanism of Action, *J Drug Des Res*, 5 (2018).
 51. Wachter VJ, Silverman JA, Zhang Y, and Benet LZ, Role of P-glycoprotein and cytochrome P450 3A in limiting oral absorption of peptides and peptidomimetics, *J Pharm Sci*, 87 (1998), 1322–30. [PubMed: 9811484]
 52. Xu L, and Desai MC, Pharmacokinetic enhancers for HIV drugs, *Curr Opin Investig Drugs*, 10 (2009), 775–86.
 53. Midde NM, Gong YQ, Cory TJ, Li JH, Meibohm B, Li WH, and Kumar S, Influence of Ethanol on Darunavir Hepatic Clearance and Intracellular PK/PD in HIV-Infected Monocytes, and CYP3A4-Darunavir Interactions Using Inhibition and in Silico Binding Studies, *Pharm Res-Dordr*, 34 (2017), 1925–33.
 54. Buss N, Snell P, Bock J, Hsu A, and Jorga K, Saquinavir and ritonavir pharmacokinetics following combined ritonavir and saquinavir (soft gelatin capsules) administration, *Br J Clin Pharmacol*, 52 (2001), 255–64. [PubMed: 11560557]
 55. Xu LH, Liu HT, Murray BP, Callebaut C, Lee MS, Hong A, Strickley RG, Tsai LK, Stray KM, Wang YJ, Rhodes GR, and Desai MC, Cobicistat (GS-9350): A Potent and Selective Inhibitor of Human CYP3A as a Novel Pharmacoenhancer, *Acs Med Chem Lett*, 1 (2010), 209–13. [PubMed: 24900196]
 56. Lo MC, Aulabaugh A, Jin G, Cowling R, Bard J, Malamas M, and Ellestad G, Evaluation of fluorescence-based thermal shift assays for hit identification in drug discovery, *Anal Biochem*, 332 (2004), 153–9. [PubMed: 15301960]
 57. Miyazaki Y, Doi N, Koma T, Adachi A, and Nomaguchi M, Novel In Vitro Screening System Based on Differential Scanning Fluorimetry to Search for Small Molecules against the Disassembly or Assembly of HIV-1 Capsid Protein, *Front Microbiol*, 8 (2017), 1413. [PubMed: 28791001]
 58. Pantoliano MW, Petrella EC, Kwasnoski JD, Lobanov VS, Myslik J, Graf E, Carver T, Asel E, Springer BA, Lane P, and Salemme FR, High-density miniaturized thermal shift assays as a general strategy for drug discovery, *J Biomol Screen*, 6 (2001), 429–40. [PubMed: 11788061]
 59. Adachi A, Gendelman HE, Koenig S, Folks T, Willey R, Rabson A, and Martin MA, Production of acquired immunodeficiency syndrome-associated retrovirus in human and nonhuman cells transfected with an infectious molecular clone, *J Virol*, 59 (1986), 284–91. [PubMed: 3016298]
 60. Schrödinger Small-Molecule Drug Discovery Suite 2019–1, Schrödinger, LLC, New York, NY, 2019.
 61. Schrödinger Release 2019–1: Maestro, Schrödinger, LLC, New York, NY, 2019.
 62. Sastry GM, Adzhigirey M, Day T, Annabhimoju R, and Sherman W, Protein and ligand preparation: parameters, protocols, and influence on virtual screening enrichments, *J Comput Aid Mol Des*, 27 (2013), 221–34.
 63. Jorgensen WL, Maxwell DS, and TiradoRives J, Development and testing of the OPLS all-atom force field on conformational energetics and properties of organic liquids, *J Am Chem Soc*, 118 (1996), 11225–36.
 64. Schrödinger Release 2019–1: LigPrep, Schrödinger, LLC, New York, NY, 2019.
 65. Friesner RA, Banks JL, Murphy RB, Halgren TA, Klicic JJ, Mainz DT, Repasky MP, Knoll EH, Shelley M, Perry JK, Shaw DE, Francis P, and Shenkin PS, Glide: a new approach for rapid,

accurate docking and scoring. 1. Method and assessment of docking accuracy, *J Med Chem*, 47 (2004), 1739–49. [PubMed: 15027865]

Author Manuscript

Author Manuscript

Author Manuscript

Author Manuscript

Highlights

- Design of novel analogs and sub-chemotypes of HIV-1 CA-targeting antiviral **PF74**.
- 5-Hydroxyindole analogs (**8,9** and **12**) showed much improved potency over **PF74**
- 2-Indolone analogs (**16-24**) decreased the T_m of CA hexamers
- The potencies of α - and β -naphthyl analogs (**33** and **27**) were comparable to **PF74**

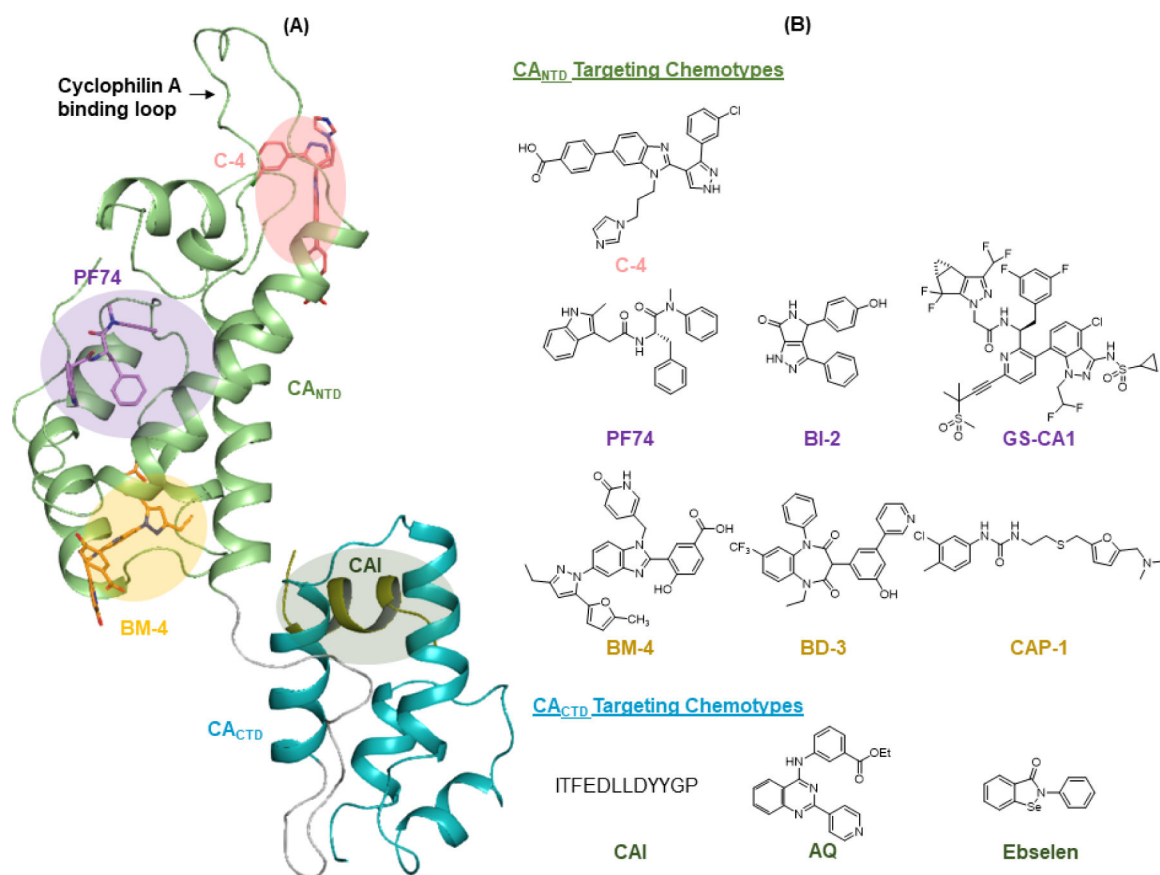


Figure 1. Compound binding sites and chemotypes targeting HIV-1 CA. (A) Ligand binding sites. Three distinct small molecule binding sites at CA_{NTD} are known for C-4, **PF74** and BM-4, respectively. Host factor cyclophilin A binds to the loop on top. Polypeptide CAI binds to the CA_{CTD}. Binding modes were reproduced in Maestro based on PDB 4XFZ [30] with ligands C-4 & BM-4 (PDB: 4E92 [31]) and CAI (PDB: 2BUO [32]) aligned. The picture was created in PyMOL while shadows of binding sites were rendered in PowerPoint; (B) major chemotypes binding to each site: BI-2 and GS-CA1 bind to the **PF74** site; BD-3 and CAP-1 bind to the BM-4 site; arylquinazoline (AQ) and ebselen bind to CA_{CTD}.

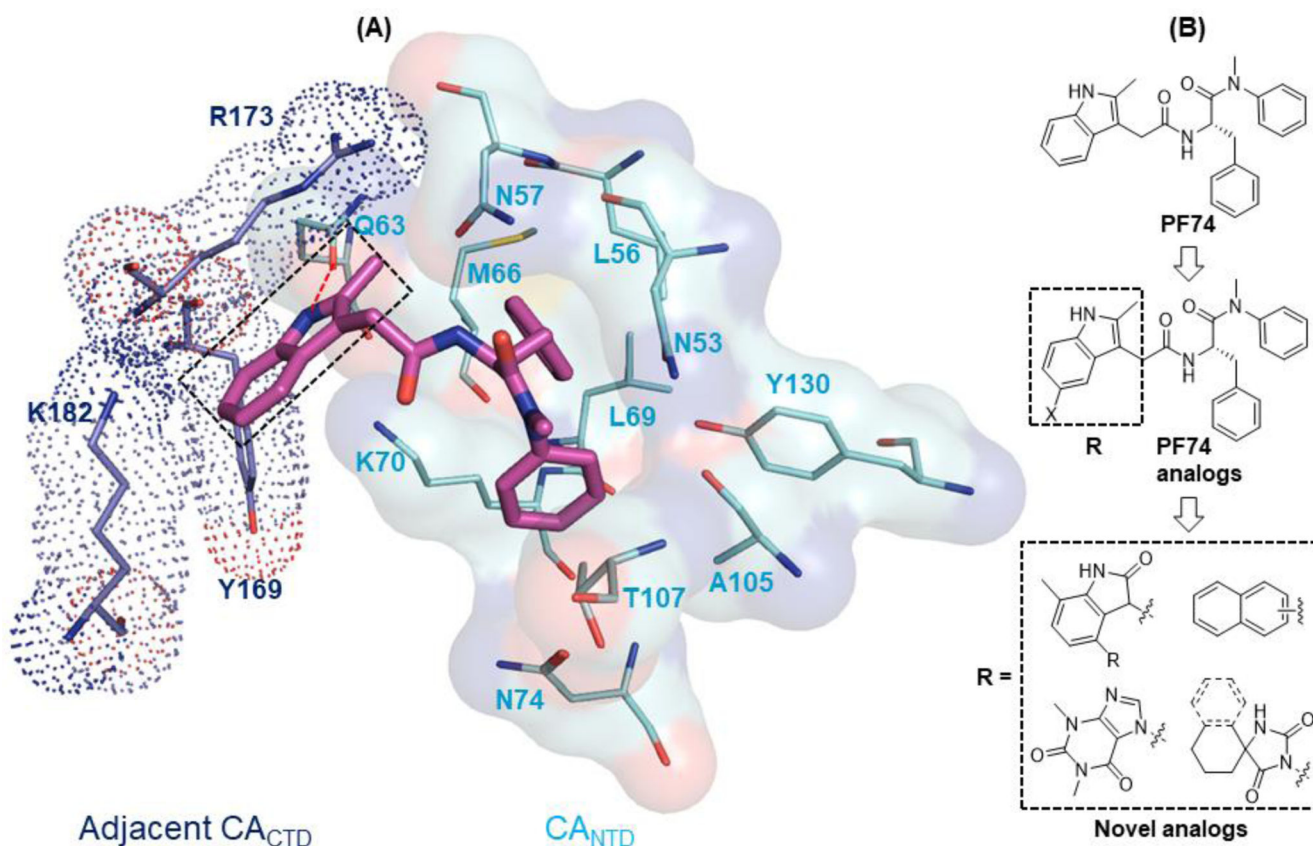


Figure 2. Binding mode of **PF74** based on PDB 4XFZ [30] and the design of novel analogs. (A) Detailed molecular interaction network of **PF74** (magenta sticks) with residues (lines) in both the CA_{NTD} (transparent cyan surface) and the adjacent CA_{CTD} (blue dot). The indole moiety of **PF74** (boxed) interacts with Q63, K70 of CA_{NTD} and Y169, R173, and K182 of the adjacent CA_{CTD}; (B) Novel analogs designed to explore the two-domain interactions of the indole moiety.

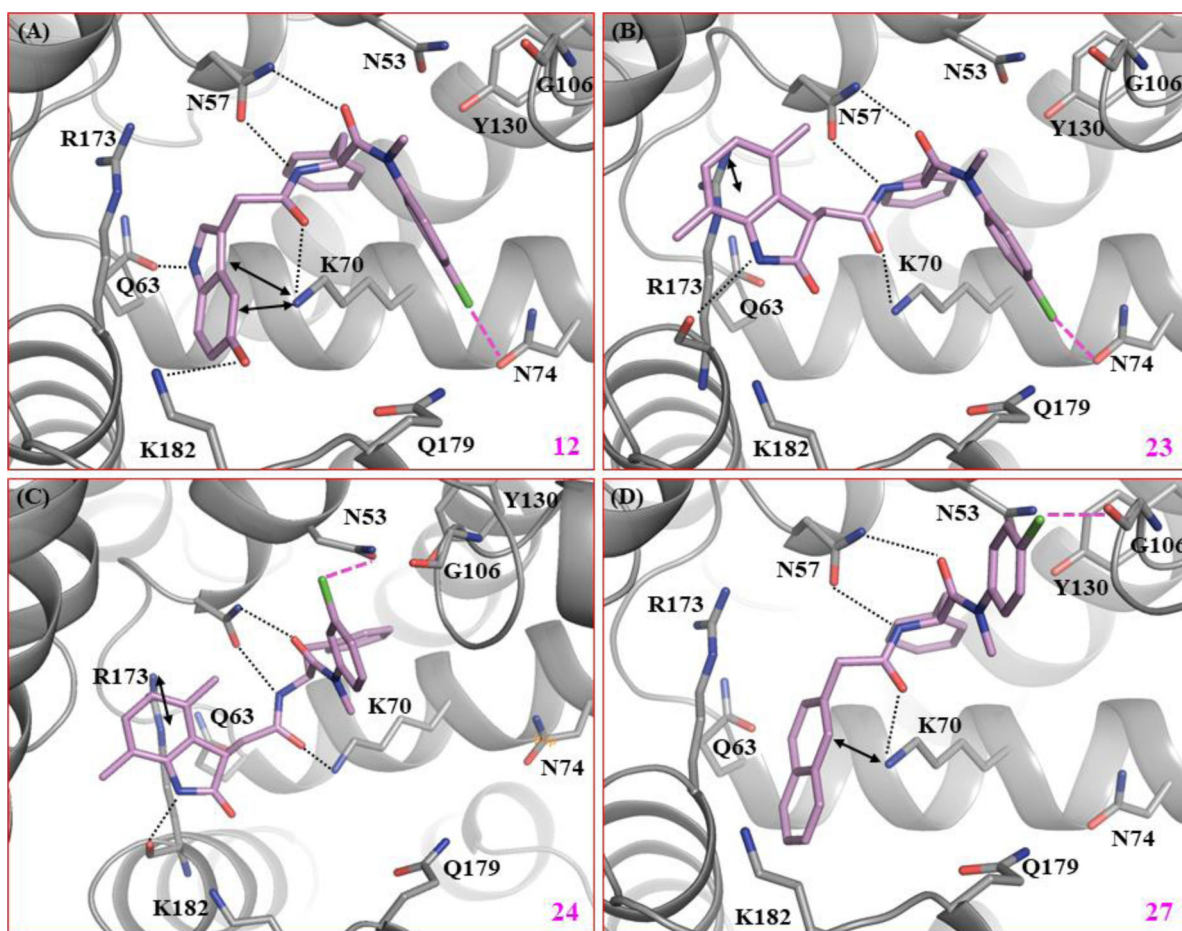
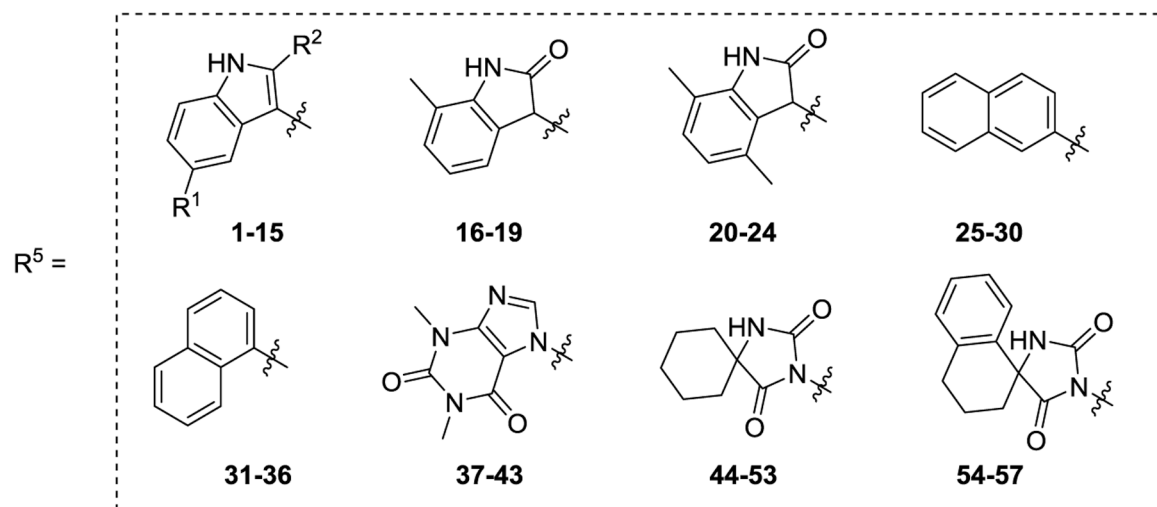
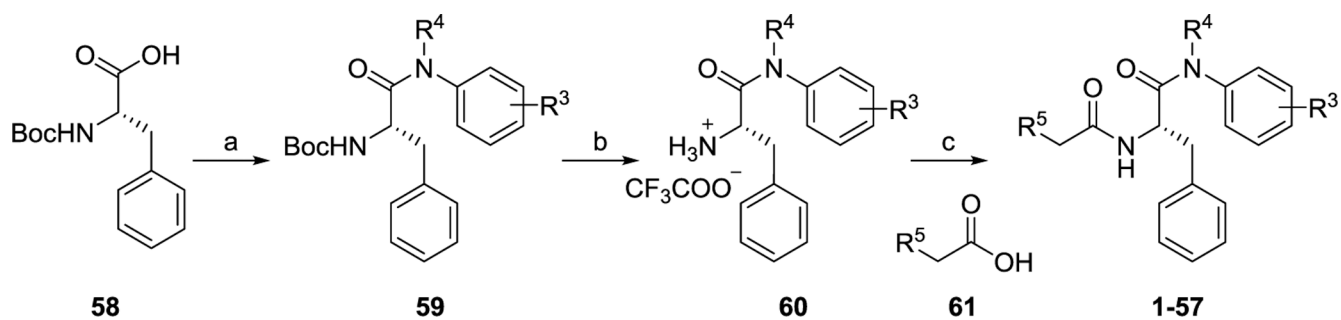


Figure 3. Docking poses of key compounds based on native HIV-1 capsid protein bound to **PF74** (Glide score: -5.8) (PDB code: 4XFZ [30]). (A) Predicted binding mode of compound **12** (Glide score: -7.6 kcal/mol). (B) Predicted binding mode of **23** (Glide score: -6.4 kcal/mol). (C) Predicted binding mode of **24** (Glide score: -6.8 kcal/mol). (D) Predicted binding mode of **27** (Glide score: -6.1 kcal/mol). Hydrogen-bonding, halogen-bonding and cation- π interactions are depicted as black dotted lines, pink dashed lines, and double headed arrows, respectively. CA with key residues around the binding site, and ligands **12**, **23**, **24**, and **27** are colored grey and violet, respectively. The nitrogen, oxygen, and chlorine atoms are colored blue, red, and green, respectively.

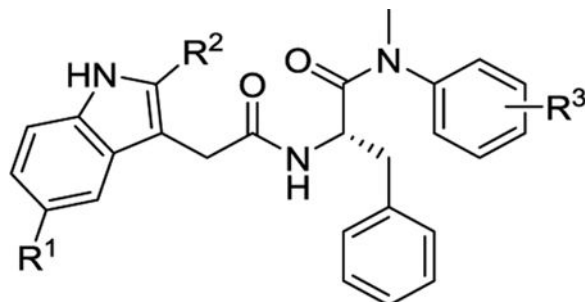


Scheme 1. Synthesis of novel PF74 analogs.

Reagents and conditions: (a) amine, HATU (or T₃P), DIPEA, DMF, rt, 12 h; (b) TFA; DCM, rt, 4–6 h; (c) HATU, DIPEA, DMF, rt, 12 h.

Table 1.

Anti-HIV-1 activity, cytotoxicity, and CA hexamer stability profiles of **PF74** analogs (modifications at R¹, R², R³).



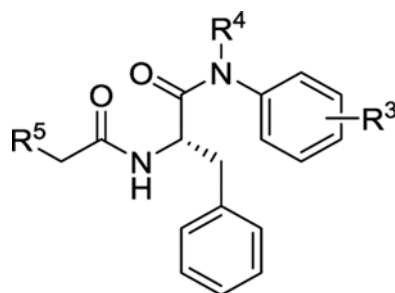
Compd	R ¹	R ²	R ³	EC ₅₀ ^a (μM)	CC ₅₀ ^b (μM)	TSA ^c	Tm (°C)
PF74 (1)	H	Me	H	0.61 ± 0.2	76 ± 9	7.4	
2	H	H	H	0.46 ± 0.1	> 100	6.1	
3	OMe	H	H	0.56 ± 0.3	48 ± 5	4.9	
4	OMe	H	4-Me	0.28 ± 0.02	> 50	5.4	
5	OMe	H	4-F	0.57 ± 0.02	> 50	6.6	
6	OMe	H	3-F	0.99 ± 0.002	> 50	4.2	
7	OMe	H	4-Cl	0.31 ± 0.02	> 50	8.0	
8	OH	H	H	0.053 ± 0.02	55 ± 2	6.8	
9	OH	H	4-Me	0.035 ± 0.004	> 100	6.3	
10	OH	H	4-F	0.46 ± 0.03	> 50	3.1	
11	OH	H	3-F	0.32 ± 0.02	47 ± 6	4.4	
12	OH	H	4-Cl	0.032 ± 0.01	> 100	6.6	
13	OH	H	3-Cl	0.31 ± 0.01	> 100	6.9	
14	OH	H	3-Br	0.38 ± 0.1	> 100	5.8	
15	OH	H	3-CF ₃	0.48 ± 0.02	65 ± 18	6.8	

^aConcentration of compound inhibiting HIV-1 replication by 50%, expressed as the mean ± standard deviation from at least two independent experiments.

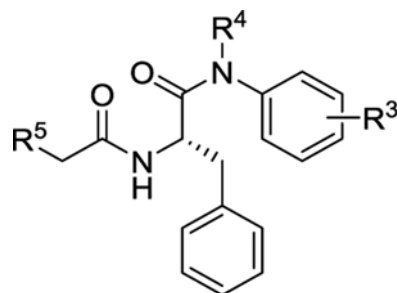
^bConcentration of compound causing 50% cell death, expressed as the mean ± standard deviation from at least two independent experiments.

^cTSA: thermal shift assay. Tm: change of CA hexamer melting point in presence of compound compared to DMSO control.

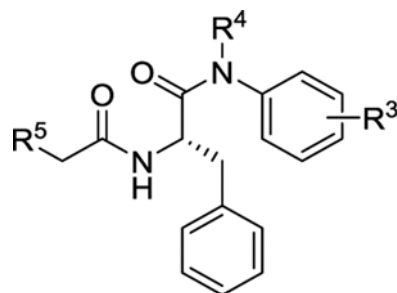
Table 2.

Anti-HIV-1 activity, cytotoxicity, and CA hexamer stability profiles of novel analogs (R³, R⁴, R⁵).

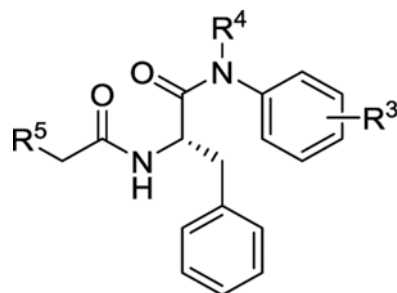
Compd	R ⁵	R ⁴	R ³	Inhibition% at 2 μM / 20 μM	EC ₅₀ ^a (μM)	CC ₅₀ ^b (μM)	TSA ^c T _m (°C)
PF74 (1)		Me	H	91/98	0.61 ± 0.2	76 ± 9	7.4
16		Me	H	0/91	ND	> 50	-1.2
17		Me	4-Cl	17/96	ND	~ 50	-0.4
18		Me	3-Cl	14/85 ^d	3.3 ± 0.3	> 100	-1.7
19		Me	3-F	0/93	ND	> 50	-0.9



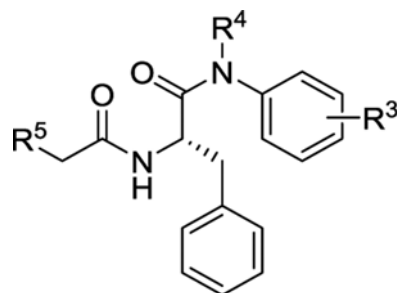
Compd	R ⁵	R ⁴	R ³	Inhibition% at 2 μ M / 20 μ M	EC ₅₀ ^a (μ M)	CC ₅₀ ^b (μ M)	TSA ^c T _m ($^{\circ}$ C)
20		Me	H	0/72 ^d	4.9 \pm 0.3	> 100	-1.8
21		Me	4-F	0/70 ^d	5.4 \pm 0.5	> 100	-1.7
22		Me	3-F	0/70 ^d	5.2 \pm 0.4	60 \pm 6	-1.8
23		Me	4-Cl	10/98 ^d	2.8 \pm 0.1	63 \pm 13	-1.3
24		Me	3-Cl	27/99 ^d	2.1 \pm 0.2	43 \pm 2	-2.4



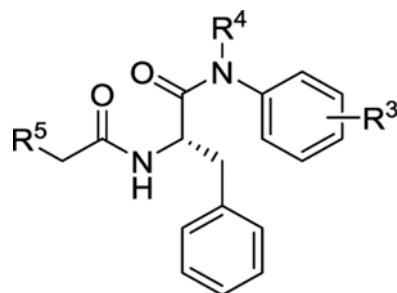
Compd	R ⁵	R ⁴	R ³	Inhibition% at 2 μM / 20 μM	EC ₅₀ ^a (μM)	CC ₅₀ ^b (μM)	TSA ^c T _m (°C)
25		Me	H	40/98	ND	< 50	4.8
26		Me	4-Me	80/99	0.99 ± 0.005	< 50	6.4
27		Me	4-Cl	95/100	0.63 ± 0.02	< 50	7.0
28		Me	3-Cl	0/94	ND	< 50	4.3
29		Me	3-F	0/97	ND	< 50	5.2
30		Et	H	46/97	ND	< 50	4.3
31		Me	H	66/100	1.1 ± 0.04	< 50	6.0



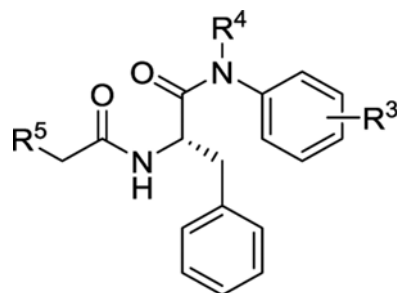
Compd	R ⁵	R ⁴	R ³	Inhibition% at 2 μM / 20 μM	EC ₅₀ ^a (μM)	CC ₅₀ ^b (μM)	TSA ^c T _m (°C)
32		Me	4-Me	96/100	1.0 ± 0.2	< 50	5.7
33		Me	4-Cl	98/100	0.83 ± 0.03	< 50	7.2
34		Me	3-Cl	53/96	ND	< 50	4.4
35		Me	3-F	44/97	ND	< 50	5.4



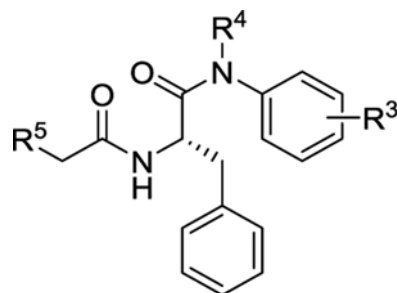
Compd	R ⁵	R ⁴	R ³	Inhibition% at 2 μ M / 20 μ M	EC ₅₀ ^a (μ M)	CC ₅₀ ^b (μ M)	TSA ^c T _m ($^{\circ}$ C)
36		Et	H	53/98	1.8 \pm 0.09	< 50	4.9
37		Me	H	10/94	ND	> 50	0.9
38		Me	4-Me	18/98	ND	> 50	1.6
39		Me	4-F	14/85	ND	> 50	0
40		Me	3-F	1/67	ND	> 50	0.5



Compd	R ⁵	R ⁴	R ³	Inhibition% at 2 μ M / 20 μ M	EC ₅₀ ^a (μ M)	CC ₅₀ ^b (μ M)	TSA ^c T _m ($^{\circ}$ C)
41		Me	4-Cl	6/96	ND	> 50	1.5
42		Me	3-Cl	0/71	ND	> 50	0
43		Et	H	0/94	ND	> 50	0.8
44		Me	H	-/89	8.9 \pm 1.5	>100	1.3
45		H	H	-/0	>20	>100	0
46		Me	4-OMe	-/93	5.1 \pm 2	>100	1.8



Compd	R ⁵	R ⁴	R ³	Inhibition% at 2 μ M / 20 μ M	EC ₅₀ ^a (μ M)	CC ₅₀ ^b (μ M)	TSA ^c T _m ($^{\circ}$ C)
47		Me	4-Me	-/92	1.9 \pm 0.5	>100	2.7
48		Me	4-F	9/99	ND	> 50	3.1
49		Me	3-F	24/98	ND	> 50	1.3
50		Me	4-Cl	-/96	2.5 \pm 0.5	>100	2.2
51		Me	3-Cl	9/98	ND	< 50	3.3
52		Me	3-Br	-/36	> 20	> 50	1.5



Compd	R ⁵	R ⁴	R ³	Inhibition% at 2 μM / 20 μM	EC ₅₀ ^a (μM)	CC ₅₀ ^b (μM)	TSA ^c T _m (°C)
53		Et	H	-/92	7.6 ± 0.9	>100	2.0
54		Me	H	-/32	> 20	> 100	0
55		H	H	-/22	> 20	> 100	0.6
56		Me	4-OMe	-/20	> 20	> 100	0.8
57		Me	4-Me	-/41	> 20	> 100	0.8

^aConcentration of compound inhibiting HIV-1 replication by 50%, expressed as the mean ± standard deviation from at least two independent experiments.

^bConcentration of compound causing 50% cell death, expressed as the mean ± standard deviation from at least two independent experiments.

^cTSA: thermal shift assay. T_m: change of CA hexamer melting point in presence of compound compared to DMSO control.

^dFor these compounds, % inhibition is reported at 1 μM / 10 μM.

Author Manuscript

Author Manuscript

Author Manuscript

Author Manuscript

Table 3.Phase I metabolic stability in liver microsomes $t_{1/2}$ (min).

Compd	HLM ^a	HLM ^a (+Cobi ^c)	MLM ^b	MLM ^b (+Cobi ^c)
PF74^c	0.7	91	0.6	34
3	1.2	--	0.5	--
7	1.8	--	0.6	--
16	7.0	--	1	--
20	1.5	--	0.6	--
24	6.7	107	1.4	34
25	1.8	--	0.5	--
27	2.7	>120	1.4	18
31	0.6	--	0.5	--
33	1.1	102	0.6	7.4
37	4.7	--	1.2	--
46	5.2	--	0.7	--
47	3.3	--	1.2	--
48	1.1	--	0.5	--
50	2.5	>120	1.1	20

^aHLM: human liver microsome^bMLM: mouse liver microsome^cMicrosomal stability measured in the presence of CYP3A inhibitor Cobi.